American Mineralogist, Volume 72, pages 39–58, 1987

Metamorphic hydrology at 13-km depth and 400–550°C

JOHN M. FERRY
Department of Earth and Planetary Sciences, Johns Hopkins University, Baltimore, Maryland 21218, U.S.A.

ABSTRACT

The progressive metamorphism of a single stratigraphic unit of impure carbonate rock from conditions of the chlorite zone to conditions of the sillimanite zone involved the following sequence of prograde reactions: muscovite + ankerite + albite → biotite + calcite + quartz + anorthite component of plagioclase; ankerite + quartz + plagioclase → calcic amphibole + calcite; biotite + calcite + quartz ± amphibole → diopside + clinozoisite + K-feldspar. Prograde mineral reactions liberated a CO_2-rich mixture of volatiles. Pressure during metamorphism was near 3500 bars (~13 km); and temperature varied between ~390°C in the chlorite zone and ~530°C in the sillimanite zone. Metacarbonate rocks were in equilibrium during metamorphism at all grades with an H_2O-rich, CO_2-H_2O fluid with X_{CO_2} = ~0.1–0.2.

The flow pattern of reactive metamorphic fluids through six large outcrops of metacarbonate rock in the chlorite, biotite, garnet, staurolite-andalusite, and sillimanite zones was determined by calculating and mapping fluid-rock ratios for numerous samples within each outcrop. Two components of fluid flow were detected: a pervasive component and a channelized component. In the chlorite, biotite, and garnet zones, fluid flow was highly channelized along bedding with enhanced flow occurring within certain layers that acted as metamorphic aquifers. A smaller but detectable amount of pervasive fluid flow occurred within the intervening layers that acted as metamorphic aquitards. Fluid-rock ratios calculated for some aquifers and aquitards in the same outcrop differed by over a factor of 50 at grades lower than the staurolite-andalusite zone. Fluid-rock ratios were uniform within any given layer over distances of up to at least ~15 m parallel to bedding. In the sillimanite zone, flow was more pervasive, and fluid-rock ratios differed by no more than a factor of 1.5 between any beds within the same outcrop. In the staurolite-andalusite zone, patterns of fluid flow were transitional between those in the sillimanite zone and those at lower grades: metamorphic aquifers and aquitards could still be identified, but the difference in their fluid-rock ratios was much less than at lower grades (less than a factor of ~6). Two generalizations can be made about the control of metamorphic grade on patterns of metamorphic fluid flow: (1) with increasing metamorphic grade, fluid flow becomes less channelized and more pervasive and (2) with increasing grade, average fluid-rock ratios increase.

INTRODUCTION

One of the most important chemical changes in rocks during metamorphism is devolatilization—the loss of certain fugitive compounds such as H_2O and CO_2. The volatile species liberated from rocks during metamorphism form a fluid phase, and the fluid flows upward owing to buoyancy forces (Walther and Orville, 1982). Walther and Wood (1984) have envisioned two mechanisms by which fluid may flow through rocks during metamorphic events. First, fluid may be segregated into fractures with spacings measured in meters or hundreds of meters. Second, flow may be pervasive with fluid moving either along grain boundaries or along fractures whose spacing is on the order of mineral grain diameters. Wood and Walther's study raises the important question of the degree to which fluid flow is channelized vs. pervasive during metamorphism. Certainly both a component of channelized and pervasive fluid flow must occur during metamorphism, but it is of utmost significance to determine the relative importance of each component. If most metamorphic fluid flow is channelized into a few major conduits, then the fluid will have minimal thermal and chemical interaction with rock as the fluid passes toward the Earth's surface. If most or a significant fraction of fluid flow is pervasive, then fluid will extensively interact both thermally and chemically with rock overlying the fluid's point of origin. The chemical and thermal interaction of rock with fluids that pervasively flow through it may have a profound effect on the metamorphic petrogenesis of the rock (Ferry, 1986a). Depending on the dom-

0003–004X/87/0102–0039$02.00

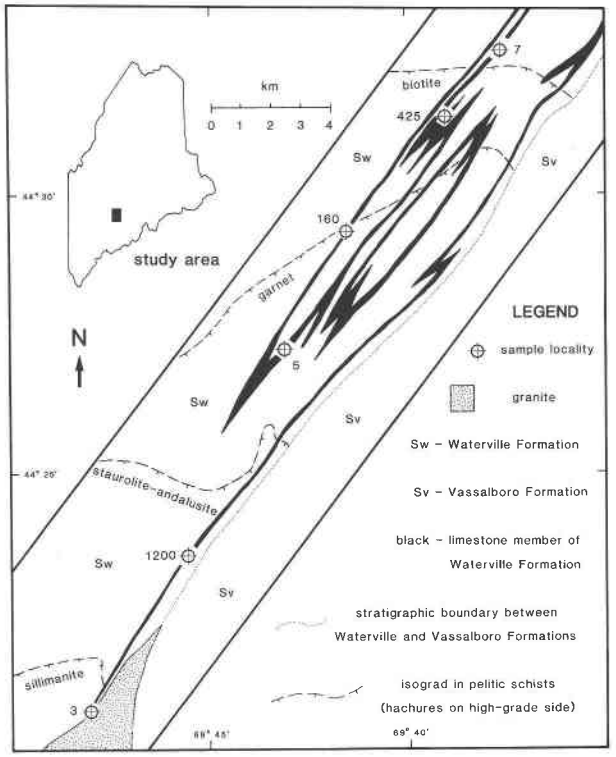

Fig. 1. Geologic sketch map of area studied. Numbers refer to sample numbers in the text. Data from Osberg (1968, 1979, pers. comm.).

inant mechanism of metamorphic fluid flow, fluid-rock interaction will be of more or less general importance during metamorphism.

If fluid infiltrates rock and is not in chemical equilibrium with it, a mineralogical record will be left of the fluid-rock interaction—a change of the rock's mineralogy caused by the chemical reaction between rock and fluid. By measuring the amount of volatiles evolved during the reaction, by estimating the composition of the fluid before reaction, and by estimating the composition of the fluid after reaction, the amount of fluid (a fluid-rock ratio) can be estimated (Ferry, 1986a). The fluid-rock ratio, therefore, serves as a natural fossil flux meter that can be used to determine directly the flow path of reactive fluid through exposures of metamorphic rock. The flux meter, however, only measures the amount of fluid that is out of chemical equilibrium with rock it infiltrates *and* that induces a chemical reaction between rock and fluid. When these conditions are met, estimated fluid-rock ratios for numerous rock samples from large outcrops can reveal whether the flow of reactive fluid was pervasive or channelized. If the flow was channelized, the nature of the channelways may be determined (e.g., mapped loci of high fluid-rock ratios may be associated with fractures, bedding, foliation, etc., in outcrop). The purpose of this study was to use fluid-rock ratios to map patterns of flow of reactive fluid in six large outcrops of metamorphosed impure carbonate rock and to determine the mechanism of fluid flow during metamorphism. The six outcrops were metamorphosed to peak conditions ranging, with reference to pelitic rocks, from chlorite grade to sillimanite grade. Changes in the mechanism of fluid flow with changing metamorphic grade therefore were also evaluated.

Geologic setting

All samples were collected from the limestone member of the Silurian Waterville Formation in south-central Maine (Fig. 1). Lithologically, the Waterville Formation is composed of interbedded shale, argillaceous limestone, argillaceous sandstone, and their metamorphic equivalents. The limestone member is distinctive for its large proportion of argillaceous carbonate rock. Because of its distinctive lithology, conclusions about metamorphic fluid flow through the limestone member of the Waterville Formation should not necessarily be generalized to the rest of the Waterville Formation or to other stratigraphic units nearby. Compositional layering is on the scale of 0.5–8 cm. The outcrop pattern of the limestone (Fig. 1) reflects isoclinally refolded recumbent folds (Osberg, 1979). Essentially all beds in the outcrops studied are vertical and strike NE–SW because of the tight isoclinal folds. Because the peak of deformation preceded the peak of metamorphism, the beds had their present orientation during the metamorphic event. Isograds based on the first appearance of biotite, garnet, staurolite + andalusite, and sillimanite in pelitic schists have been mapped by P. H. Osberg (1968 and pers. comm.). In the southern part of the map area, the Waterville Formation is intruded by synmetamorphic granitic stocks. Deformation, metamorphism, and emplacement of the stocks occurred during the Devonian Acadian orogeny (Dallmeyer and Van Breeman, 1981). Novak and Holdaway (1981) suggested that two episodes of Acadian metamorphism occurred south and west of the area represented in Figure 1. If there were two Devonian metamorphic episodes in the present area, however, they were probably closely spaced in time and in P-T conditions (Holdaway et al., 1982).

Methods of investigation

Approximately 150 samples were collected at the six outcrops whose locations are shown in Figure 1. Many samples from outcrop 5 were collected as part of an earlier study of the same stratigraphic unit (Ferry, 1979). With reference to metamorphic zones defined by the pelitic schists, samples were collected in the chlorite, biotite, garnet, staurolite + andalusite, and sillimanite zones. Each outcrop was a large exposure either in a roadcut, in a quarry, or along a stream. Consequently, numerous samples from different beds were collected along traverses up to 150 m across bedding at each outcrop. Exposures at four outcrops allowed numerous samples to be collected within beds along traverses up to 14 m parallel to bedding.

Mineral assemblages were identified by a combination of petrographic observation of thin sections and qualitative electron-microprobe analysis. Compositions of minerals in 72 samples were obtained by electron-microprobe analysis at the Geophysical Laboratory, Carnegie Institution of Washington, following methods described by Ferry (1980).

Table 1. Mineral assemblage and mineral composition data for impure carbonate rocks

Outcrop	7	7	425	425	160	160	5	5	1200	1200	3
assemblage	A	B	B	C	A	B*	B	C	B	C	D
					Major minerals						
Calcite**	0.38	0.48	0.38	0.43	0.31	0.35	0.27	0.36	0.21	0.31	0.31
Ankerite**	0.22	0.30	—	—	0.17	0.23†	0.15	0.21	—	—	—
Quartz	x	x	x	x	x	x	x	x	x	x	x
Plagioclase††	0.02	0.02	0.81	0.81	0.06	0.63	0.50	0.78	0.44	0.79	0.79
Muscovite‡	0.95	0.96	—	—	0.95	0.94†	0.94	—	0.96†	—	—
Chlorite**	0.51†	0.45	0.32	0.38	—	0.33	0.25	0.31	0.17	0.31	—
Biotite**	—	0.46	0.35	0.40	—	0.36	0.27	0.34	0.18	0.33	0.32
Amphibole**	—	—	—	0.41	—	—	—	0.33	—	0.26	0.26
Diopside**	—	—	—	—	—	—	—	—	—	—	0.24
Clinozoisite§	—	—	—	—	—	—	—	—	—	—	0.89
Microcline‡	—	—	—	—	—	—	—	—	—	—	0.95
					Accessory minerals						
Pyrrhotite‖	0.18	tr.†	0.50	0.45	0.03	0.34	0.34	0.39	0.45	0.29	0.16
Pyrite‖	0.02†	—	—	0.03†	0.03	tr.†	tr.†	0.01†	—	tr.†	—
Rutile‖	tr.†	tr.†	—	—	tr.	0.01†	0.04	—	0.13	—	—
Ilmenite‖	0.03†	0.04	—	0.05	—	0.01†	—	tr.	—	—	—
Sphene‖	—	—	0.05	—	—	—	—	—	0.13	0.23	0.23
Graphite	x	x	x	x	x	x	x	x	x	x	x
n	5	4	2	2	2	7	27	5	3	9	6

Note: x = present; — = absent; *n* = number of samples studied in detail by electron-probe microanalysis.
* One sample contains garnet with composition $(Mn_{1.42}Fe_{1.04}Ca_{0.35}Mg_{0.19})Al_2Si_3O_{12}$.
** Average atomic Fe/(Fe + Mg).
† Present in some but not all samples.
†† Average mole fraction anorthite component (7A, 7B, 160A: microprobe analysis; all others: estimated from whole-rock chemistry).
‡ Average atomic K/(K + Na).
§ Average atomic Al/(Al + Fe).
‖ Average modal percent; tr. (trace) = <0.05%.

Chemical analyses of rock samples for major-element metal oxides were performed using X-ray fluorescence methods by X-ray Assay Laboratories, Ltd., Don Mills, Ontario. Analyses for carbonate CO_2 were performed by X-ray Assay Laboratories by dissolving known quantities of rock in HCl and precipitating the evolved CO_2 as a measurable amount of $BaCO_3$.

Modal amounts of biotite, chlorite, amphibole, clinozoisite, diopside, pyrite, pyrrhotite, ilmenite, sphene, and rutile were determined in samples by counting 2000 points in thin section in both reflected and transmitted light. Volume amounts of the minerals were converted to molar amounts (per reference liter of rock) using molar volume data (Robie et al., 1967; Hewitt and Wones, 1975; McOnie et al., 1975).

Mineralogy and mineral chemistry

Mineral assemblages

Mineral assemblages observed in samples of the limestone member of the Waterville Formation from each outcrop are listed in Table 1. The mineralogy of the metamorphosed carbonate rocks was assigned to one of four different mineral assemblages.

Assemblage A. Rocks with mineral assemblage A are composed of calcite, ankerite, muscovite, quartz, and sodic plagioclase ($X_{an} < 0.12$). Accessory minerals include rutile, pyrrhotite, and graphite with and without chlorite, pyrite, and ilmenite. Assemblage A is distinguished from the other assemblages by the presence of sodic plagioclase and by the absence of biotite, amphibole, clinozoisite, diopside, and K-feldspar. Of seven samples with assemblage A, three contain chlorite and four do not. For six samples with assemblage A and coarse enough that they could be point-counted for chlorite, the modal chlorite content is in the range 0–0.05% with an average of 0.01%. Assemblage A is found in both the chlorite and garnet zones. In outcrop 7 (chlorite zone) it is the commonest assemblage (5 out of 9 samples studied in detail). In outcrop 160 it is an uncommon assemblage (2 out of 9 samples studied in detail). Assemblage A was not observed in any of the other outcrops.

Assemblage B. Rocks with mineral assemblage B are composed of calcite, biotite, chlorite, quartz, and intermediate to calcic plagioclase (X_{an} = 0.3–0.9) with and without muscovite and ankerite. Accessory minerals include pyrrhotite and graphite with and without pyrite. Rocks with assemblage B always contain one of these accessory Ti-rich phases: rutile, ilmenite, or sphene. Three samples with assemblage B from outcrop 1200 contain both rutile and sphene. Assemblage B is distinguished from the other assemblages by the presence of biotite and by the absence of amphibole, diopside, clinozoisite, and K-feldspar. Rocks with assemblage B most commonly contain both muscovite and ankerite (35 out of 40 samples studied in detail); less common are rocks with muscovite but not ankerite (2 of 40 samples), with ankerite but not muscovite (1 of 40 samples), and with neither muscovite nor ankerite (2 of 40 samples). Of 40 samples with assemblage B, 37 contain chlorite and 3 do not. For 33 samples with assemblage B that were counted for chlorite, the modal chlorite content is in the range 0–3.4% with an average of 0.35%. Although outcrop 7 is in the chlorite zone with respect to assemblages observed in pelitic schists, 4 of 9 metacarbonate rocks studied in detail from the outcrop contain assemblage B with biotite. In outcrops 425, 160, and 5 (biotite and garnet zones), assemblage B is the commonest observed (40 out of 47 samples studied in detail). In outcrop 1200 (staurolite-andalusite zone), assemblage B is uncommon (3 out of 12 samples), and it is absent from outcrop 3 (sillimanite zone).

Assemblage C. Rocks with mineral assemblage C are composed of calcite, biotite, calcic amphibole, chlorite, quartz, and calcic plagioclase with and without ankerite. Accessory minerals

Table 2. Average composition of carbonates and silicates in each type of mineral assemblage from each outcrop

	Calcites											Ankerites					
Outcrop	7	7	425	425	160	160	5	5	1200	1200	3	7	7	160	160	5	5
Assemblage	A	B	B	C	A	B	B	C	B	C	D	A	B	A	B	B	C
Ca	0.933	0.916	0.946	0.926	0.930	0.915	0.940	0.923	0.951	0.952	0.977	1.005	1.011	1.005	1.014	1.011	1.019
Fe	0.020	0.029	0.017	0.021	0.014	0.019	0.015	0.023	0.010	0.010	0.004	0.204	0.275	0.152	0.213	0.144	0.203
Mg	0.032	0.032	0.028	0.028	0.031	0.036	0.040	0.041	0.038	0.022	0.009	0.740	0.629	0.769	0.711	0.827	0.743
Mn	0.016	0.024	0.009	0.025	0.025	0.030	0.006	0.014	0.002	0.015	0.010	0.051	0.086	0.074	0.062	0.019	0.036

	Muscovites						Biotites								
Outcrop	7	7	160	160	5	1200	7	425	425	160	5	5	1200	1200	3
Assemblage	A	B	A	B	B	B	B	B	C	B	B	C	B	C	D
K	0.848	0.874	0.890	0.900	0.888	0.873	0.837	0.793	0.837	0.845	0.856	0.809	0.842	0.888	0.909
Na	0.041	0.038	0.042	0.054	0.054	0.035	0.005	0.008	0.001	0.009	0.012	0.010	0.017	0.016	0.005
Fe	0.080	0.132	0.063	0.057	0.049	0.037	1.123	0.875	0.977	0.855	0.652	0.868	0.455	0.812	0.804
Mg	0.189	0.209	0.197	0.139	0.154	0.188	1.329	1.619	1.512	1.531	1.774	1.675	2.063	1.684	1.677
Mn	—	0.001	0.001	—	—	—	0.008	0.004	0.014	0.013	0.003	0.004	—	0.015	0.022
Ti	0.020	0.017	0.036	0.027	0.026	0.030	0.091	0.079	0.079	0.086	0.076	0.081	0.060	0.077	0.053
Al	1.759	1.698	1.734	1.800	1.797	1.775	0.345	0.336	0.317	0.396	0.373	0.309	0.321	0.309	0.330
Al	0.833	0.800	0.832	0.892	0.875	0.847	1.224	1.203	1.200	1.238	1.180	1.206	1.129	1.198	1.163
Si	3.167	3.200	3.168	3.108	3.125	3.153	2.776	2.797	2.800	2.762	2.820	2.794	2.871	2.802	2.837

	Chlorites									Amphiboles				Diopside	Clinozoisite
Outcrop	7	7	425	425	160	5	5	1200	1200	425	5	1200	3	3	3
Assemblage	A	B	B	C	B	B	C	B	C	C	C	C	D	D	D
K	—	—	—	—	—	—	—	—	—	0.024	0.022	0.031	0.046	—	—
Na	—	—	—	—	—	—	—	—	—	0.222	0.231	0.147	0.104	0.012	—
Ca	—	—	—	—	—	—	—	—	—	1.802	1.801	1.897	1.973	0.979	2.001
Fe	2.265	2.039	1.466	1.693	1.499	1.139	1.439	0.776	1.413	1.726	1.425	1.194	1.247	0.236	0.319
Mg	2.214	2.500	3.074	2.785	3.039	3.432	3.198	3.856	3.161	2.527	2.946	3.422	3.514	0.748	0.011
Mn	0.039	0.024	0.012	0.031	0.032	0.004	0.011	—	0.037	0.094	0.037	0.071	0.071	0.022	0.011
Ti	0.003	0.007	0.003	0.007	0.005	0.004	0.005	0.005	0.005	0.062	0.039	0.035	0.008	0.001	0.005
Al	2.767	2.678	2.683	2.702	2.685	2.665	2.624	2.552	2.648	1.804	1.747	1.001	0.615	0.037	2.635
Si	2.649	2.683	2.689	2.689	2.681	2.698	2.962	2.752	2.692	6.789	6.806	7.277	7.545	1.966	3.019

Note: Calcite: cations/1 oxygen atom (excluding CO_2); ankerite: cations/2 oxygen atoms (excluding CO_2); muscovite and biotite: cations/11 oxygen atoms (excluding H_2O); chlorite: cations/14 oxygen atoms (excluding H_2O); amphibole: cations/23 oxygen atoms (excluding H_2O); diopside: cations/6 oxygen atoms; zoisite: cations/12.5 oxygen atoms (excluding H_2O). All Fe in calcite, ankerite, muscovite, biotite, chlorite, and diopside as ferrous; all Fe in zoisite as ferric; ferrous/ferric ratio in amphibole adjusted so Fe + Mg + Mn + Ti + Al + Si = 13 per standard amphibole formula unit.

include pyrrhotite and graphite with and without pyrite. Rocks with assemblage C always contain either accessory sphene or ilmenite but never both. One sample contains rutile + sphene. Assemblage C is distinguished from the other assemblages by the presence of calcic amphibole and by the absence of muscovite, diopside, clinozoisite, and K-feldspar. In outcrops 425 and 1200, all samples with assemblage C lack ankerite. In outcrop 5, on the other hand, all samples with assemblage C contain ankerite. In outcrops 425 and 5, the accessory Ti-rich mineral in assemblage C is ilmenite, whereas in outcrop 1200, it is sphene. All 16 samples with assemblage C contain chlorite, and their modal chlorite content is in the range <0.05–1.2% with an average of 0.46%. Assemblage C was not observed in the chlorite or sillimanite zones (outcrops 7 and 3, respectively). It is an uncommon assemblage in the biotite and garnet zones (observed in 7 out of 47 samples studied in detail from outcrops 425, 160, and 5). Assemblage C is the commonest assemblage in metacarbonate rocks from the staurolite-andalusite zone (9 out of 12 samples studied in detail from outcrop 1200).

Assemblage D. Rocks with mineral assemblage D are composed of calcite, biotite, calcic amphibole, diopside, clinozoisite, K-feldspar, quartz, and calcic plagioclase. Accessory minerals always include pyrrhotite, sphene, and graphite. Assemblage D is distinguished from the other assemblages by the presence of diopside, clinozoisite, and K-feldspar and by the absence of muscovite, ankerite, and chlorite. Assemblage D was observed only in the sillimanite zone (outcrop 3), and every sample studied in detail from outcrop 3 contained assemblage D.

Prograde sequence of mineral assemblages. Assemblage A occurs in approximately half of the samples from the chlorite zone but is uncommon or absent in outcrops at higher grade. Assemblage B is common in the biotite and garnet zones but less common or absent in the chlorite, staurolite-andalusite, and sillimanite zones. Assemblage C is common in the staurolite-andalusite zone but not in the chlorite, biotite, garnet, or sillimanite zones. Assemblage D is found exclusively in the sillimanite zone. The prograde sequence of mineral assemblages that developed in metamorphosed carbonate rocks from the Waterville Formation therefore appears to have been A → B → C → D. The occurrence of ankerite + calcic amphibole and the absence of muscovite + calcic amphibole and of ankerite + diopside + clinozoisite + K-feldspar suggest the following general order in which minerals were developed and then were destroyed in the carbonate rocks during progressive metamorphism: (1) formation of biotite and intermediate to calcic plagioclase, (2) disappearance of muscovite, (3) formation of calcic amphibole, (4) disappearance of ankerite, and (5) formation of diopside + clinozoisite + K-feldspar. Only rocks from the sillimanite zone experienced the entire evolutionary sequence, and different rocks from the same outcrop may represent different stages in the sequence. Samples from the same outcrop but with different mineral assemblages experienced different degrees of progress of the same set of prograde mineral-fluid reactions.

Mineral chemistry

Table 2 contains the average measured composition of carbonates and silicates in each mineral assemblage, A–D, from each outcrop.

Table 3. Representative whole-rock chemical analyses of carbonate rocks of each type of mineral assemblage from each outcrop

Outcrop	7	7	425	425	160	160	5	5	1200	1200	3
Assemblage	A	B	B	C	A	C	B	C	B	C	D
Sample number	7-A1	7-G1	425-E1	425-K1	160-L	160-D	5-AA2	5-DD2	1200-B	1200-G	3-D1
SiO_2	18.4	25.5	14.7	25.3	18.3	17.8	22.2	23.6	22.2	23.6	22.2
TiO_2	0.14	0.31	0.17	0.33	0.12	0.15	0.21	0.33	0.19	0.28	0.25
Al_2O_3	2.85	7.45	4.60	8.43	2.37	4.23	3.80	8.31	3.51	5.76	6.52
Fe_2O_3	1.39	8.70	3.51	7.89	1.60	2.35	2.10	5.99	1.44	2.55	3.43
MgO	1.92	3.89	2.41	4.72	2.53	2.55	3.66	5.23	2.18	3.40	3.60
MnO	0.26	0.94	0.36	1.24	1.35	1.10	0.26	0.54	0.11	0.09	0.68
CaO	39.6	27.3	39.2	27.3	38.7	37.8	34.4	29.4	38.2	35.3	35.0
Na_2O	0.77	0.20	0.19	0.42	0.41	0.15	0.62	0.30	0.43	0.64	0.26
K_2O	0.35	0.89	1.02	1.05	0.35	1.02	0.70	1.70	0.64	1.13	1.67
P_2O_5	0.04	0.09	0.08	0.24	0.04	0.05	0.05	0.14	0.06	0.06	0.05
LOI	33.7	24.8	32.2	22.0	33.7	32.5	31.6	23.3	30.8	26.8	25.3
Total	99.4	100.1	98.4	99.0	99.5	99.7	99.6	98.8	99.8	99.6	99.0
CO_2	32.8	22.9	32.7	18.6	34.1	29.6	32.0	23.7	34.4	27.6	24.3

Note: Values in weight percent; all Fe as Fe_2O_3; LOI = loss on ignition.

Carbonates. Analyzed calcites are characterized by Ca ≫ Mg > Fe > Mn. Although Ca contents of calcites within an outcrop may vary by up to 0.05 atoms per CO_2-free oxygen atom, there is a systematic increase in the average Ca content of calcites from ~0.93 to ~0.98 per standard formula unit between the chlorite and sillimanite zones. Ankerite is close to a $Ca(Mg,Fe,Mn)(CO_3)_2$ solid solution with Mg ≫ Fe ≫ Mn. Analyzed ankerites principally differ only in Fe/(Fe + Mg) (cf., Ferry, 1979, Fig. 4); which may vary by up to ~0.2 among ankerites from the same outcrop. The range in Fe/(Fe + Mg) of ankerites from an individual outcrop is comparable to the range in Fe/(Fe + Mg) of all analyzed ankerites from the chlorite, biotite, and garnet zones.

Feldspars. Analyzed plagioclase from assemblage A is sodic ($X_{an} < 0.12$). Analyzed plagioclase from the same thin section of rocks with assemblages B, C, and D in the biotite zone and at higher grades is more calcic: plagioclase in 48 of 52 such analyzed samples has a composition in the range $X_{an} = 0.29$–0.84. Furthermore, analyzed plagioclases in the same thin section are usually chemically heterogeneous; their compositions may differ by up to 0.4 X_{an}. The effect has been noted before for plagioclase from this same stratigraphic unit (Ferry, 1979). The variation in composition is interpreted in terms of a miscibility gap in the plagioclase solid solution series at the conditions of metamorphism (Grove et al., 1983). Rocks with assemblages B, C, and D probably contain aggregates of coexisting plagioclase feldspars, $\sim An_{30}$ + $\sim An_{85}$, intergrown on a very fine scale. The variation in analyzed plagioclase composition may be the result of analyzing mixtures with different proportions of the two coexisting feldspars.

K-feldspar in assemblage D is microcline with a very limited range in composition, $Or_{94}Ab_6$–$Or_{96}Ab_4$.

Sheet silicates. Analyzed muscovites deviate from the ideal composition principally by incorporation of the paragonite and phengite components in solid solution. The paragonite content of muscovites does not differ appreciably among samples from the same outcrop and does not significantly change as a function of metamorphic grade. The average phengite content of muscovites from the chlorite zone is greater than at higher grades. The range in phengite content of muscovites from individual outcrops in the biotite, garnet, and staurolite-andalusite zones is comparable to the entire range in measured phengite contents of micas at grades higher than the chlorite zone.

Analyzed biotites deviate from the ideal composition of phlogopite principally by the incorporation of Ti and by the Fe-Mg and (Fe,Mg)Si-2Al substitution schemes. The range in Ti contents of biotites from individual outcrops in the chlorite, biotite, garnet, and staurolite-andalusite zones is comparable to the entire range in Ti contents of biotites of all samples from the four zones. On the average, biotites from the sillimanite zone, however, contain distinctly less Ti than do biotites from lower grades. The Ti content of all analyzed biotites is small (< ~0.1 atom per 11 anhydrous oxygen atoms), and their Al contents are quite uniform. Within individual outcrops, the major variation in biotite composition is in the Fe/(Fe + Mg) ratio (cf., Ferry, 1979, Fig. 3), which may differ by up to ~0.2. The range in Fe/(Fe + Mg) of biotites from individual outcrops is comparable to the range in Fe/(Fe + Mg) of all analyzed biotites from all outcrops. The average Fe/(Fe + Mg) of biotite from outcrop 7, however, is distinctly greater than the average Fe/(Fe + Mg) of biotite from each of the other outcrops at higher grades.

Analyzed chlorites are repidolites with quite uniform Al contents. Within individual outcrops, the major variation in chlorite composition is in the Fe/(Fe + Mg) ratio (cf., Ferry, 1979, Fig. 3), and it may vary by up to ~0.2. The range in Fe/(Fe + Mg) of chlorites for individual outcrops is comparable to the range in Fe/(Fe + Mg) of all analyzed chlorites from all outcrops. The average Fe/(Fe + Mg) of chlorite from outcrop 7, however, is distinctly greater than average Fe/(Fe + Mg) of chlorite from each of the other outcrops at higher grades.

Muscovites, biotites, and chlorites from outcrop 5 described by Ferry (1979, Table 1) have a greater range in Fe/(Fe + Mg) (up to ~0.4) than those reported in this study. Phyllosilicates from the outcrop with Fe/(Fe + Mg) > ~0.35 are exclusively found in the rare assemblage muscovite + biotite + chlorite + garnet + plagioclase + calcite + quartz + pyrrhotite + graphite. Because no samples of this assemblage were used in this study, the range in Fe/(Fe + Mg) of phyllosilicates for assemblages considered (garnet-free assemblages B and C) is much less, ~0.2.

Chain silicates. Analyzed calcic amphiboles are either tschermakitic hornblendes, magnesio-hornblendes, actinolitic hornblendes, or actinolites in the nomenclature of Leake (1978). The compositions of analyzed amphiboles from outcrop 5 are uniform (cf., Ferry, 1979, Fig. 4, Table 1). Analyzed amphiboles from outcrops 425, 1200, and 3, on the other hand, exhibit large variations in composition among samples from the same outcrop [Na and Al contents, Fe/(Fe + Mg)]. Nevertheless, some general trends in amphibole composition as a function of metamorphic grade are evident. Tschermakitic hornblendes are re-

Table 4. Mean and standard deviation of whole-rock atomic values of *i*/Al for all analyzed carbonate rocks from each outcrop

	Outcrop 7		Outcrop 425		Outcrop 160		Outcrop 5		Outcrop 1200		Outcrop 3	
i/Al	Mean	S.D.	Mean	S.D.	Mean	S.D.	Mean	S.D.	Mean	S.D.	Mean	S.D.
Si/Al	3.936	1.353	3.479	1.124	3.679	1.898	3.670	1.452	3.651	1.304	3.005	0.436
Ti/Al	0.025	0.003	0.025	0.004	0.027	0.004	0.030	0.005	0.029	0.005	0.024	0.001
Fe/Al	0.537	0.162	0.475	0.126	0.401	0.077	0.347	0.071	0.400	0.125	0.396	0.129
Mg/Al	0.770	0.153	0.738	0.155	0.754	0.268	0.807	0.140	0.791	0.132	0.797	0.145
Ca/Al	8.760	4.216	7.391	3.785	6.274	5.474	5.895	3.701	6.284	2.976	5.230	1.371
Na/Al	0.181	0.164	0.074	0.065	0.130	0.089	0.131	0.068	0.130	0.082	0.078	0.020
K/Al	0.195	0.071	0.235	0.080	0.237	0.046	0.227	0.054	0.229	0.058	0.264	0.075
n	12		13		12		34		18		7	

Note: S.D. = standard deviation; *n* = number of samples analyzed.

stricted to the biotite zone, whereas actinolites are restricted to the staurolite-andalusite and sillimanite zones. The patterns of occurrence reflect the decrease in average Na and octahedral Al contents and in Fe/(Fe + Mg) of analyzed amphiboles with increasing metamorphic grade.

Analyzed diopsides are close to $Ca(Fe,Mg)Si_2O_6$ solid solutions with Fe/(Fe + Mg) in the range 0.20–0.29.

Clinozoisite. Analyzed clinozoisite is close to a $Ca_2(Al,Fe)_3Si_3O_{12}(OH)$ solid solution with Al/(Al + Fe) in the restricted range 0.88–0.91.

Accessory minerals. Analyzed rutile is close to pure TiO_2, and analyzed sphene is close to pure $CaTiSiO_5$. No analyses were obtained of accessory pyrrhotite, pyrite, ilmenite, or graphite.

Whole-rock chemistry

Major-element chemical analyses were obtained for 96 rock samples collected from the six outcrops shown in Figure 1. Representative analyses of rocks with each assemblage type from each outcrop are listed in Table 3. In order to compare the composition of rocks from different outcrops, some basis for comparison must be established. Following earlier practice (Carmichael, 1969; Thompson, 1975; Ferry, 1983a) a constant-Al reference frame was adopted that is justified by the low solubility of Al in aqueous fluids (Frantz et al., 1981). Consequently the ratios of the concentrations of major elements to that of Al were calculated for all analyzed samples and expressed on an atomic basis. Table 4 compiles the average atomic whole-rock Si/Al, Ti/Al, Fe/Al, Mg/Al, Ca/Al, Na/Al, and K/Al values for all analyzed specimens from the same outcrop.

The limestone member of the Waterville Formation is chemically heterogeneous. Nevertheless, results in Table 4 suggest that relative to Al, the average concentration of Si, Ti, Fe, Mg, and Ca of metacarbonate rock from each outcrop is not significantly different from the average concentration of corresponding elements in metacarbonates from the other outcrops. There is no firm evidence from the whole-rock analyses for any change in the Si, Ti, Fe, Mg, and Ca contents of the metacarbonate rocks with increasing grade of metamorphism.This conclusion is supported by an earlier whole-rock chemical study of impure carbonate rocks from the adjacent Vassalboro Formation that found no positive evidence for change in Si, Ti, Fe, Mg, or Ca contents relative to Al during progressive metamorphism (Ferry, 1983a). Data from the earlier study, however, indicate that average metacarbonate rock from the chlorite zone of the Vassalboro Formation contains ~5 times more K and ~3 times more Na than do average rocks from the highest grades. In contrast, mean K/Al ratios of carbonate rocks from the six outcrops of the limestone member of the Waterville Formation are remarkably similar. Furthermore, the standard deviations of mean K/Al values are relatively small. Unlike rocks from the Vassalboro Formation, there is no positive evidence from the whole-rock chemical data for loss of K from the metacarbonates of the Waterville Formation with progressive metamorphism. The case for Na loss is less definite. The mean Na/Al ratio of carbonate rocks from outcrop 7 is distinctly greater than the mean Na/Al ratio for all outcrops at higher grades. Taken at face value, the mean Na/Al ratios in Table 4 suggest loss of over 50% Na from some metacarbonates during the metamorphic event. The mean value of Na/Al for each outcrop, however, is within one standard deviation of mean Na/Al for the other outcrops, and the standard deviations are large. Data suggest but do not require loss of Na from rocks of the limestone member of the Waterville Formation with increasing grade of metamorphism. Based on results in Table 4 and the study of Ferry (1983a), it is assumed that progressive metamorphism of the limestone member of the Waterville Formation was isochemical with respect to Al, Si, Ti, Fe, Mg, Ca, and K. The possibility for some loss of Na from the rocks during metamorphism, however, cannot be dismissed.

The chemical behavior of the limestone member of the Waterville Formation was different from the behavior of argillaceous carbonate rocks in the adjacent Vassalboro Formation (Ferry, 1983a). At the highest grades exposed, carbonate rocks from the Vassalboro Formation lost, on the average, >70% of both their Na and K. The loss of alkalis was attributed to hydrolysis reactions that proceeded in rocks from the Vassalboro Formation during the metamorphic event. Rocks from the limestone member of the Waterville Formation, on the other hand, show no positive evidence for loss of K. The difference in the chemical response of the two rock units to metamorphism, in turn, implies that metamorphic fluids that attended metamorphism of the Vassalboro Formation were characterized (for unknown reasons) by much lower K/H than those that attended metamorphism of the Waterville Formation.

Physical conditions during metamorphism

Pressure and temperature

Pressure. Based on measurements using four different geobarometers, pressure was estimated at 3500 bars during metamorphism of the Waterville Formation in the staurolite-andalusite and sillimanite zones (Ferry, 1980). Pressure was assumed to be 3500 bars throughout the exposed area of the Waterville Formation shown in Figure 1. The depth of metamorphism therefore was ~13 km.

Temperature. Peak metamorphic temperatures recorded by eight different geothermometers in rocks from the Waterville

Table 5. Thermochemical data and activity-composition relations used in the calculation of metamorphic fluid composition

Reaction	$\Delta\bar{H}$ (J)	$\Delta\bar{S}$ (J/deg)	$\Delta\bar{V}_s$ (J/bar)	Source
(1) $KAl_3Si_3O_{10}(OH)_2 + 2SiO_2 + CaCO_3 = KAlSi_3O_8 + CaAl_2Si_2O_8 + CO_2 + H_2O$	183 694	353.481	−1.318	Hewitt (1973)
(2) $5KMg_3AlSi_3O_{10}(OH)_2 + 6CaCO_3 + 24SiO_2 = 3Ca_2Mg_5Si_8O_{22}(OH)_2 + 5KAlSi_3O_8 + 6CO_2 + 2H_2O$	651 926	1269.108	−15.171	Hoschek (1973)
(3) $KAlSi_3O_8 + 3CaMg(CO_3)_2 + H_2O = KMg_3AlSi_3O_{10}(OH)_2 + 3CaCO_3 + 3CO_2$	223 095	428.099	−4.058	Puhan (1978)
(4) $TiO_2 + CaCO_3 + SiO_2 = CaTiSiO_5 + CO_2$	83 086	165.921	−2.280	Jacobs and Kerrick (1981)
(5) $2Ca_2Al_3Si_3O_{12}(OH) + CO_2 = 3CaAl_2Si_2O_8 + CaCO_3 + H_2O$	55 840	103.148	+6.623	Allen and Fawcett (1982)
(6) $KAl_3Si_3O_{10}(OH)_2 + 3CaMg(CO_3)_2 + 2SiO_2 = KMg_3AlSi_3O_{10}(OH)_2 + CaAl_2Si_2O_8 + 2CaCO_3 + 4CO_2$	406 789	781.580	−5.376	Reaction 1 + Reaction 3
(7) $5CaMg(CO_3)_2 + 8SiO_2 + H_2O = Ca_2Mg_5Si_8O_{22}(OH)_2 + 3CaCO_3 + 7CO_2$	589 132	1136.533	−11.820	⅓[(5 × Reaction 3) + Reaction 2]

Note: Activity-composition relations as follows: Muscovite, biotite, and calcite—same as Ferry (1976). Plagioclase—Carpenter and Ferry (1984). Rutile, quartz, and sphene—pure substances with unit activity. Ankerite—$a_{CaMg(CO_3)_2}$ = [Mg], zoisite—$a_{Ca_2Al_3Si_3O_{12}(OH)}$ = [Al] − 2, and amphibole—$a_{Ca_2Mg_5Si_8O_{22}(OH)_2}$ = $[v_A][Ca/2]^2[Mg/5]^5$, where [*i*] = number of atoms *i* per standard formula unit in Table 2 and v_A = atom fraction vacancy in amphibole A site.

Formation have been recently reviewed by Ferry (1986b). The preferred temperature of the sillimanite, staurolite-andalusite, garnet, and biotite isograds (Fig. 1) are ~520, ~475, ~430, and ~400°C, respectively. By interpolating between these temperatures or by extrapolating them slightly to grades higher than the sillimanite isograd and to grades lower than the biotite isograd, peak metamorphic temperatures were assigned to each of the six outcrops shown in Figure 1: outcrop 3, 530°C; outcrop 1200, 490°C; outcrop 5, 450°C; outcrop 160, 430°C; outcrop 425, 410°C; outcrop 7, 390°C. These values are consistent with earlier published temperature estimates for both pelitic schists and impure carbonate rocks from the Waterville Formation (e.g., Ferry, 1979, 1980, 1984).

Fluid composition

Earlier estimates of the composition of C-O-H-S fluid in equilibrium during metamorphism with carbonate rocks of the Waterville Formation indicated that, for practical purposes, the fluid was a binary CO_2-H_2O mixture (Ferry, 1976, 1979). The composition of fluid in equilibrium with mineral assemblages from five of the outcrps was therefore estimated assuming $p_{CO_2} + p_{H_2O} = P_{total} = 3500$ bars, following the general procedures outlined by Ferry and Burt (1982) and specifically using their Equation 39. Table 5 summarizes the mineral equilibria used to estimate metamorphic fluid composition as well as the pertinent thermochemical parameters and activity-composition models for the minerals. Fugacity coefficients for H_2O and CO_2 were taken from Burnham et al. (1969) and Burnham and Wall (pers. comm.), respectively. Ideal mixing of CO_2 and H_2O in the metamorphic fluid was assumed. Pressure-temperature conditions of mineral-fluid equilibrium were taken as those estimated above. Calculated results are summarized in Table 6.

Outcrop 5. Seventeen analyzed samples containing muscovite + ankerite + quartz + biotite + calcite + plagioclase record X_{CO_2} at 450°C in the narrow range of 0.14–0.16. Six analyzed samples containing ankerite + quartz + calcic amphibole + calcite record equilibrium X_{CO_2} = 0.13–0.16 at 450°C. Ferry (1979) reported that one sample containing ankerite + quartz + calcic amphibole + calcite recorded X_{CO_2} = 0.59. The calculated result, based on thermochemical data of Skippen (1974), is in error because the term $2.303R(2000)$ was mistakenly dropped when Skippen's values of A^*, B^*, and C^* were recalculated as values of $\Delta\bar{H}$, $\Delta\bar{S}$, and $\Delta\bar{V}_s$. Correctly using Skippen's thermochemical data, rather than those in Table 5 of this paper, the six analyzed samples with ankerite + quartz + amphibole + calcite record X_{CO_2} = 0.14–0.15 at 450°C in good agreement with results in Table 6.

The calculated values of X_{CO_2} in Table 6 and Figure 2, while representing preferred estimates, are subject to error from a number of sources: errors in estimated thermochemical parameters, errors in activity-composition relations for minerals and fluid, errors in fugacity coefficients, and errors in estimated temperature and pressure of equilibrium. The stated uncertainty in Skippen's thermochemical parameters translate into an uncertainty in X_{CO_2} of ±0.08 recorded by ankerite + quartz + amphibole + calcite. Skippen's A^*, B^*, and C^* values for the dolomite-quartz-tremolite-calcite equilibrium were estimated from A^*, B^*, C^* values of four other equilibria, and values of $\Delta\bar{H}$ and $\Delta\bar{S}$ for the equilibrium in Table 5 were obtained from $\Delta\bar{H}$ and $\Delta\bar{S}$ of only two other equilibria. Uncertainties in calculated values of X_{CO_2} in Table 6 for ankerite-quartz-amphibole-calcite, owing to uncertainties in $\Delta\bar{H}$ and $\Delta\bar{S}$, therefore are probably less than the ±0.08 indicated from uncertainties in Skippen's thermochemical parameters. In general, however, these errors are difficult or impossible to evaluate (particularly in the case of activity-composition relations), and a rigorous error analysis of

Table 6. Calculated composition of CO_2–H_2O fluid in equilibrium with carbonate rock during metamorphism

Outcrop	7	160	5	5	1200	1200	3
Assemblage	B	B	B	C	B	C	D
No. of samples	3	2	17	6	3	1	6
X_{CO_2}	0.070–0.074	0.106	0.140–0.160	0.134–0.157	0.235–0.236	0.240	0.079–0.096
Equilibrium*	a	a	a	b	c	c	d

* a = muscovite-ankerite-quartz-biotite-calcite-plagioclase-fluid; b = dolomite-quartz-amphibole-calcite-fluid; c = rutile-calcite-quartz-sphene-fluid; d = zoisite-calcite-plagioclase-fluid.

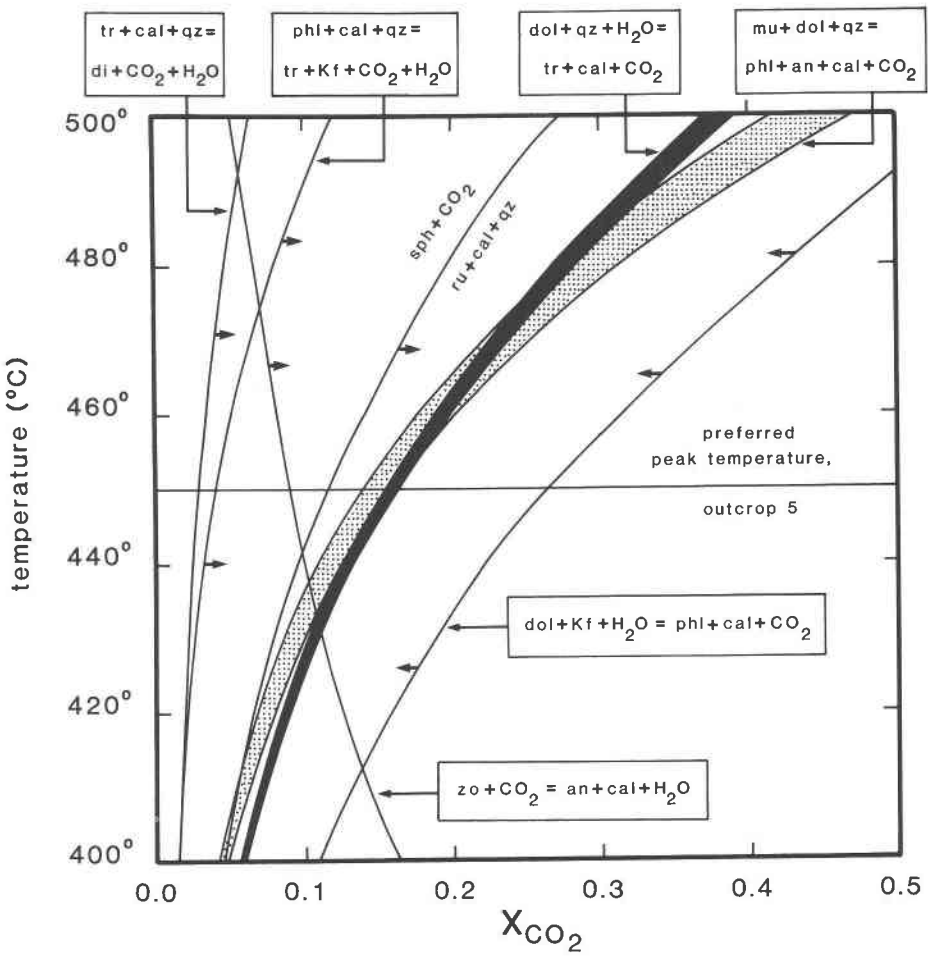

Fig. 2. T-X_{CO_2} diagram illustrating mineral-fluid equilibria pertinent to observed mineral assemblages in metacarbonate rocks from outcrop 5, Fig. 1. Abbreviations: an = anorthite, cal = calcite, zo = zoisite, phl = phlogopite, dol = dolomite, Kf = potassium feldspar, mu = muscovite, qz = quartz, ru = rutile, sph = sphene, tr = tremolite, di = diopside, am = amphibole. Black and stippled areas: range in T-X_{CO_2} conditions consistent with range in measured mineral compositions for the observed assemblages ankerite + quartz + amphibole + calcite and muscovite + ankerite + quartz + biotite + calcite + plagioclase, respectively. Values of $\Delta\bar{H}$, $\Delta\bar{S}$, and $\Delta\bar{V}_s$ used to calculate curves either from Table 5 of this study or from Ferry (1976). For curves other than mu + dol + qz = phl + cal + an and dol + qz = am + cal, quartz, rutile, sphene, and zoisite were assumed pure substances with unit activity; K-feldspar was assumed $Or_{95}Ab_{05}$; calcite was assumed $Ca_{0.93}(Fe,Mg,Mn)_{0.07}CO_3$; amphibole and biotite were assumed to have the average composition of those minerals in analyzed samples from outcrop 5; diopside was assumed to be $Ca(Fe,Mg)Si_2O_6$ in Fe-Mg exchange equilibrium with average amphibole in outcrop 5. Activity-composition relationships were those in Table 5. Heavy short arrows point to the side of the curve on which observed mineral assemblages in outcrop 5 are stable.

calculated X_{CO_2} is not possible and was not attempted. Two considerations, however, support calculated values of X_{CO_2} in Table 6. First, calculated values of X_{CO_2} are consistent with other pertinent mineral-fluid equilibria shown in Figure 2. At temperatures near 450°C, the T-X_{CO_2} curves for observed assemblages muscovite + ankerite + quartz + biotite + calcite + plagioclase and ankerite + quartz + amphibole + calcite lie at higher values of X_{CO_2} than do curves for the equilibria (a) rutile-calcite-quartz-sphene, (b) zoisite-calcite-plagioclase, (c) biotite–calcite–quartz–amphibole–K-feldspar, and (d) amphibole-calcite-quartz-diopside and at lower values of X_{CO_2} than does the curve for ankerite–K-feldspar–biotite–calcite, all consistent with the presence of rutile, calcite, quartz, plagioclase, biotite, and calcic amphibole in rocks from outcrop 5 and with the absence of sphene, clinozoisite, K-feldspar, and diopside. Second, the narrow range in calculated X_{CO_2} is consistent with the results of an earlier study that utilized a completely different sort of analysis. Ferry (1979) showed that during metamorphism, the chemical potential of CO_2 differed significantly—by up to 104 calories—among samples from outcrop 5. New data from this study extends the limit to ~125 calories. In terms of X_{CO_2}, a difference of 125 calories in μ_{CO_2} corresponds to a difference of ~10% relative X_{CO_2} (i.e., absolute differences of ~0.01–0.02 for values of X_{CO_2} = 0.1–0.2). Calculated differences in X_{CO_2} in Table 6 match those implied by the differences in μ_{CO_2} calculated by Ferry (1979).

Once values of pressure, temperature, and thermochemical parameters are chosen and once fugacity coefficients and a mixing model for the fluid species is specified, the only parameter that affects variations in calculated X_{CO_2} for samples from the same outcrop is K_s, the activity product for the solid phases in

the equilibrium of interest. For 17 samples from outcrop 5, ln K_s for equilibrium 6, Table 5, is in the narrow range −3.6 to −5.8. For 6 samples from outcrop 5, ln K_s for equilibrium 7, Table 5, is in the narrow range −6.2 to +7.9. Alternative activity-composition relations for the mineral solid solutions are not likely to greatly change the magnitude of the range in ln K_s values. Values of ln K_s are small relative to $\Delta\bar{S}$ of equilibria 6 and 7. Regardless, therefore, of exact values of T, P, $\Delta\bar{H}$, $\Delta\bar{S}$, $\Delta\bar{V}_s$, and fugacity and activity coefficients chosen to calculate X_{CO_2}, the range in calculated X_{CO_2} recorded by samples from outcrop 5 must be small.

Outcrops 7 and 160. Three analyzed samples from outcrop 7 and two analyzed samples from outcrop 160 contain the assemblage muscovite + ankerite + quartz + biotite + calcite + plagioclase. The range in ln K_s for equilibrium 6, Table 5, is between −16.9 and −17.8 for samples from outcrop 7 and between −4.85 and −4.94 for samples from outcrop 160. Given the preferred values of pressure and temperature at the two outcrops, of thermochemical parameters for the equilibrium, and of fugacity coefficients, the range in calculated X_{CO_2} is <0.01 for both outcrops with estimated X_{CO_2} = 0.07 at outcrop 7 and X_{CO_2} = 0.11 at outcrop 160. Regardless of any error in the absolute value of the calculated X_{CO_2}, the small range in ln K_s values in outcrops 7 and 160 suggests that fluid composition varied little within the two outcrops during metamorphism.

Outcrop 1200. Four samples from outcrop 1200 contain the assemblage rutile + calcite + quartz + sphene, and the range in ln K_s for equilibrium 4, Table 5, is 0.3–0.5. Calculated values of X_{CO_2} differ by <0.01, and the average value is 0.24. The remaining samples from outcrop 1200 do not contain mineral assemblages from which X_{CO_2} can be calculated with confidence. The other samples, however, contain sphene without rutile, requiring that the equilibrium fluid was characterized by X_{CO_2} less than that defined by equilibrium 4, Table 5 (i.e., <0.24 at 490°C). The presence of biotite + calcite + quartz and the absence of K-feldspar in rocks from outcrop 1200, however, limits X_{CO_2} of the equilibrium fluid at 490°C to values >~0.1 (Fig. 2).

Outcrop 3. The six analyzed samples from outcrop 3 contain plagioclase + calcite + clinozoisite, and the range in ln K_s for equilibrium 5, Table 5, is 1.42–2.3. Calculated values of X_{CO_2} are in the range 0.08–0.10.

Discussion. Two generalizations can be made from the calculations of fluid composition. First, there appears to have been surprisingly small variation in equilibrium fluid composition within each outcrop even though the outcrops contain different mineral assemblages and even though the compositions of minerals from different samples having the same assemblage are significantly different. Because small variations in fluid composition within a given outcrop are ultimately based on small variations in measured ln K_s values for various mineral equilibria, the conclusion will not be changed by alternative choices for metamorphic temperature and pressure, thermochemical parameters, fugacity coefficients, etc. Furthermore, significant but small variations in fluid composition have been verified for the outcrop investigated in greatest detail (outcrop 5) by an analysis that is independent of the one used in this study (Ferry, 1979). Second, calculated values of X_{CO_2} in Table 6 suggest that the fluid was H_2O-rich (i.e., in the range X_{CO_2} = ~0.1–0.2) at all stages of prograde metamorphism in the area.

Prograde mineral reactions

The sequence of prograde mineral reactions that occurred in individual samples of metacarbonate rock was determined by (1) calculating the moles of minerals that now compose 1 L of each rock sample; (2) calculating the moles of minerals of each lower-grade assemblage that earlier composed that same quantity of rock, assuming metamorphism was isochemical for all major metallic elements except, in some instances, Na; and (3) calculating the sequence of prograde reactions from the difference in moles of minerals in each succeeding pair of metamorphic assemblages for each sample.

Calculated mineral abundances

Assemblage B. The volume amounts (modes) of biotite, chlorite, rutile, sphene, ilmenite, pyrrhotite, and pyrite were determined in each sample by counting 2000 points in thin section. Volume amounts were converted to molar amounts (per reference liter of rock) using molar-volume data and compositions of the minerals. The fine-grained texture of the rocks precluded direct determination of modal amounts of muscovite, calcite, ankerite, quartz, and plagioclase by point counting. The molar amount of muscovite, calcite, ankerite, quartz, and $CaAl_2Si_2O_8$ (An) and $NaAlSi_3O_8$ (Ab) components in plagioclase in each sample was therefore calculated using a set of mass-balance equations of the form

$$i/\mathrm{Al} = \left[\sum_j \alpha_{i,j} n_j\right] \Big/ \left[\sum_j \alpha_{\mathrm{Al},j} n_j\right], \tag{1}$$

where i/Al is calculated on an atomic basis (obtained from whole-rock chemical data like that summarized in Table 3), $\alpha_{i,j}$ is the number of atoms of element i per standard formula unit of mineral j (obtained from mineral analyses like those summarized in Table 2), and n_j is the number of moles of mineral j per liter of rock. For assemblage B, n_j = 13, of which 6 are unknown. The six unknown n_j terms were calculated from a set of five applications of Equation 1 utilizing measured values of Na/Al, K/Al, Si/Al, Ca/Al, and (Fe + Mg + Mn)/Al for each sample and the requirement that the volume of rock that contains the minerals is 1 L, i.e.,

$$\sum_j n_j \bar{V}_j = 1000, \tag{2}$$

where $\bar{V}_j$ is the molar volume of j in cubic centimeters. Examples of calculated results for a representative sample with assemblage B from each outcrop are listed in Table 7A.

The precursor of assemblage B was assemblage A, muscovite + ankerite + calcite + quartz + albite with combinations of the accessory minerals chlorite, pyrrhotite, pyrite, graphite, rutile, and ilmenite. Accessory pyrrhotite, pyrite, graphite, rutile, and ilmenite occur in very small concentrations in rocks with assemblage A (Table 1) and therefore could be considered, without introducing significant error, to have been inert during the transition from assemblage A to assemblage B. Rocks with assemblage A contain 0–0.05 modal percent chlorite with an average of 0.01%. Chlorite is a negligible constituent of the precursors to rocks with assemblage B; the precursors to assemblage B therefore were assumed to contain no chlorite. Amounts of muscovite, ankerite, calcite, quartz, and $NaAlSi_3O_8$ in the biotite-free precursors to rocks with assemblage B were calculated assuming that metamorphism was isochemical with respect to Al, Si, Ca, Fe, Mg, Mn, and K:

$$\left[\sum_j \alpha_{i,j} n_j\right]_{\text{assemblage B}} = \left[\sum_j \alpha_{i,j} n_j\right]_{\text{assemblage A}}, \tag{3}$$

Table 7. Calculated and measured abundances of minerals in representative carbonate rocks of each type of mineral assemblage from each outcrop

Outcrop	7	425	160	5	1200	425	5	1200	3
assemblage	B	B	B	B	B	C	C	C	D
Sample no.	7-G1	425-E1	160-D	5-AA2	1200-B	425-K1	5-DD2	1200-G	3-D1
				A. Present mineral abundances (moles/liter)					
Biotite	0.086	0.783	0.156	0.488	0.325	0.767	1.262	0.733	0.316
Muscovite	0.510	—	0.516	tr.	0.108	—	—	—	—
Calcite	8.110	20.107	19.207	17.044	19.102	13.179	14.379	16.841	15.602
Ankerite	4.958	—	0.775	0.825	—	—	0.207	—	—
Quartz	7.048	2.984	5.250	6.563	6.924	2.669	3.343	4.629	0.173
Plagioclase	1.369	0.751	0.366	0.930	0.718	0.907	1.195	1.252	1.094
Amphibole	—	—	—	—	—	0.897	0.235	0.131	0.316
Diopside	—	—	—	—	—	—	—	—	1.244
K-feldspar	—	—	—	—	—	—	—	—	0.764
Clinozoisite	—	—	—	—	—	—	—	—	0.073
Chlorite	0.007	tr.	0.010	0.017	0.017	tr.	0.043	tr.	—
Pyrite	—	—	tr.	tr.	—	—	0.021	—	—
Pyrrhotite	tr.	0.283	tr.	0.339	0.198	0.198	0.226	0.226	0.057
Rutile	—	—	tr.	tr.	0.106	—	—	—	—
Sphene	—	tr.	—	—	0.009	—	—	0.036	0.027
Ilmenite	tr.	—	—	—	—	0.032	tr.	—	—
				B. Mineral abundances in assemblage A precursors (moles/liter)*					
Muscovite	0.591	0.682	0.659	0.465	0.414	0.748	1.152	0.741	1.155
Calcite	9.307	18.732	19.050	16.069	18.493	9.250	10.874	15.339	15.007
Ankerite	5.076	1.856	1.182	2.089	0.857	5.911	4.791	2.412	3.436
Quartz	2.387	2.606	4.533	6.398	6.443	1.425	2.905	5.100	5.236
Plagioclase	2.521	0.701	0.522	0.845	0.760	2.922	1.550	1.124	0.616

C. Mineral abundances in assemblage B precursors (moles/liter)*

Sample no.	425-K1	5-DD2	1200-G	3-D1
Biotite	0.808	1.269	0.742	1.106
Calcite	9.600	13.112	16.448	16.815
Ankerite	3.978	1.549	0.629	0.798
Quartz	5.819	4.397	5.527	5.038
Plagioclase	2.034	1.483	1.291	1.148

D. Mineral abundances in assemblage C precursors (moles/liter)*

Sample no.	3-D1
Amphibole	0.164
Biotite	1.096
Calcite	17.345
Quartz	3.972
Plagioclase	1.093

* With reference to 1-L present rock.

where in assemblage B, j = biotite, muscovite, chlorite, ankerite, calcite, quartz, $NaAlSi_3O_8$, $CaAl_2Si_2O_8$, sphene, ilmenite, pyrite, and pyrrhotite; in assemblage A, j = muscovite, ankerite, calcite, quartz, $NaAlSi_3O_8$, ilmenite, pyrite, and pyrrhotite; and i = Al, Si, Ca, K, and (Fe + Mg + Mn). The $\alpha_{i,j}$ were taken either from the composition of each mineral in the rock or, in the case of rocks with assemblage B that lack muscovite and/or ankerite, the average composition of muscovite and ankerite in rocks with assemblage B from outcrop 5 (Table 3). Mean whole-rock atomic Na/Al for all samples of assemblage B without muscovite (i.e., those samples of B in which the A → B transition is complete) is 0.107 (standard deviation, 0.096), whereas the mean Na/Al for all samples of assemblage A is 0.258 (standard deviation, 0.167). Although the mean values are within one standard deviation of each other, the large difference in mean Na/Al strongly suggests that the assemblage A precursors, on the average, had greater Na contents. To allow for this possible difference in Na content, assemblage A precursors were calculated conserving Al, Si, Ca, K, Fe, Mg, and Mn but not Na. The calculations, however, do not *a priori* require any difference between the Na contents of samples with assemblage B and their precursors. Applications of Equation 3 are only expressions of mass balance for Al, Si, Ca, K, and (Fe + Mg + Mn) that do not necessarily conserve either volume or Na. Calculated precursors to assemblage B therefore contain the same quantity of Al, Si, Ca, K, Fe, Mg, and Mn as does 1 L of each sample of assemblage B, but the calculated precursors, in general, have both different volumes (usually >1 L) and different Na contents (usually greater). The greater calculated Na contents of assemblage A precursors confirm suggestions based on whole-rock chemical data that carbonate rocks from the limestone member of the Waterville Formation lost Na during progressive metamorphism. Examples of assemblage A that were calculated as precursors to representative samples composed of assemblage B are listed in Table 7B.

Assemblage C. The number of moles of minerals that compose rocks with assemblage C were determined using methods similar to those used for rocks with assemblage B. Modes of calcic amphibole, chlorite, sphene, ilmenite, pyrrhotite, and pyrite were counted directly. Amounts of biotite, calcite, ankerite, quartz, and plagioclase were calculated from a set of Equations 1 and 2. Examples of calculated results for a representative sample with assemblage C from each outcrop are listed in Table 7A.

The immediate precursor of assemblage C in these samples was assemblage B without muscovite. Accessory ilmenite, pyrite, and pyrrhotite were assumed to have been inert during the transition from assemblage B to assemblage C. The modal chlorite content of rocks with assemblage B is in the range 0–3.4% with an average of 0.35%. For simplicity, precursors to assemblage C were assumed to contain no chlorite. The mean whole-rock atomic ratio Na/Al for all samples with assemblage C is 0.095 (standard deviation, 0.058), whereas mean Na/Al for samples of assemblage B that lack muscovite is 0.107 (standard deviation, 0.096). Apparently samples with assemblage B and those with assemblage C, on the average, have Na contents that are not significantly different. Assemblage B precursors to samples with assemblage C were calculated from a set of equations analogous

to Equation 3 using methods similar to those used for calculation of assemblage A precursors to rocks with assemblage B but with an additional Equation 3 for i = Na. Examples of assemblage B that were calculated as precursors to representative samples composed of assemblage C are listed in Table 7C.

Amounts of minerals in precursors to rocks with assemblage C that contain assemblage A were calculated as described previously for rocks with assemblage B, and representative examples are listed in Table 7C.

Assemblage D. The number of moles of minerals that compose rocks with assemblage D were determined using methods similar to those used for rocks with assemblages B and C. Modes of biotite, calcic amphibole, clinozoisite, pyrrhotite, and sphene were counted directly. Amounts of diopside, calcite, quartz, K-feldspar, and plagioclase were calculated from a set of Equations 1 and 2. An example of calculated results for a representative sample with assemblage D is listed in Table 7A.

The immediate precursor to assemblage D was assemblage C without ankerite. Accessory pyrrhotite was assumed to be inert during the transition from assemblage C to assemblage D. The modal chlorite content of rocks with assemblage C is in the range <0.05–1.2% with an average of 0.46%. For simplicity, the precursors of rocks with assemblage D were assumed to contain no chlorite. The mean whole-rock atomic Na/Al for all samples of assemblage D is 0.078 (standard deviation, 0.020), whereas mean Na/Al for samples of assemblage C is 0.095 (standard deviation 0.058). Apparently samples with assemblage D and those with assemblage C, on the average, have Na contents that are not significantly different. Assemblage C precursors to samples with assemblage D were calculated from a set of equations like Equation 3 using methods similar to those used for calculation of assemblage B precursors to rocks with assemblage C. An example of an assemblage C that was calculated as a precursor to a representative sample of assemblage D is listed in Table 7D.

Amounts of minerals in precursors to rocks with assemblage D that contain assemblages A and B were calculated as described previously for rocks with assemblages B and C, and representative examples are listed in Table 7B and C.

Prograde mineral reactions

The net mineralogical change by which assemblage B developed in 1 L of a particular rock sample from assemblage A is

$$\left(\sum_j n_j\right)_{\text{assemblage B}} - \left(\sum_j n_j\right)_{\text{assemblage A}} = 0, \qquad (4)$$

where the sum is taken over all minerals j that occur in a rock with assemblage B (from data like that in Table 7A) and over all minerals j that occur in its calculated precursor with assemblage A (data like that in Table 7B). For simplicity, the reactions exclude minor or trace ilmenite, pyrrhotite, pyrite, rutile, and graphite by assumption. The components $NaAlSi_3O_8$ and $CaAl_2Si_2O_8$ are entered separately into the equations rather than combined as "plagioclase." These net mineralogical changes were converted to mineral-fluid reactions by balancing them for Na, Cl, C, and H with the fluid species NaCl, HCl, H_2O, and CO_2. The resulting reactions do not represent mineral equilibria but only describe mass transfer among minerals and fluid within a reference quantity of rock that is composed of assemblage B and that occupies 1 L. Representative mineral-fluid reactions are listed in Table 8. The reactions in Table 8 are balanced for all major-element oxides but do not conserve volume. They result in a decrease in volume of the solid phases. Reactions corresponding to the transitions assemblage B → assemblage C and assemblage C → assemblage D were calculated by equations similar to Equation 4; representative examples are listed in Table 8.

Typically the transition from assemblage A to assemblage B during prograde metamorphism involved the formation of biotite, calcite, quartz, and $CaAl_2Si_2O_8$ at the expense of muscovite, ankerite, and $NaAlSi_3O_8$. A small amount of chlorite may also be produced (<0.02 mol/L). The transition from assemblage B to assemblage C typically involved the formation of calcic amphibole and calcite at the expense of ankerite, quartz, and plagioclase. Biotite and chlorite are minor participants in the reaction. The transition from assemblage C to assemblage D typically involved the formation of diopside, clinozoisite, K-feldspar, and sphene at the expense of biotite, calcite, and quartz. Calcic amphibole and plagioclase were produced in some samples and consumed in others during the C → D transition. Pyrite, pyrrhotite, ilmenite, rutile, and graphite occur in such small concentrations in the metacarbonate rocks that the minerals' participation in the prograde mineral reactions could not be determined with confidence.

Chemical interaction between carbonate rocks and aqueous fluid during prograde metamorphism

Metamorphism of impure carbonate rocks often involves the liberation of a CO_2-rich mixture of volatiles while the rock is in equilibrium with H_2O-rich fluid (Rice and Ferry, 1982; Ferry, 1983b, 1986a). The difference between the composition of volatiles that are generated by the carbonate rocks and the composition of fluid recorded by mineral assemblages has been interpreted in terms of chemical interaction of carbonate rocks with aqueous fluid during the metamorphic event. Chemical interaction between carbonate rocks and aqueous fluid has been unequivocally verified in several integrated petrologic–stable isotope investigations of both contact and regionally metamorphosed impure carbonate rocks (Rumble et al., 1982; Tracy et al., 1983; Nabelek et al., 1984; Bebout and Carlson, 1986).

It is assumed that the mass-balance relations in Table 8 correspond to prograde mineral-fluid reactions. The prograde reactions in the limestone member of the Waterville Formation liberated a CO_2-rich mixture of volatiles. In contrast, mineral assemblages in the carbonate rocks record chemical equilibrium with H_2O-rich fluids with $X_{CO_2} < 0.2$ (Table 6). Massive metacarbonates from the Waterville Formation therefore are another example of rocks that chemically interacted with aqueous fluids during their metamorphism. If reaction occurred at an invariant point in the absence of fluid-rock interaction, the composition of fluid released by the reactions must have been precisely the same as the composition of fluid with which the rock was in chemical equilibrium (Rice and Ferry, 1982; Ferry, 1983c). Results in Tables 6 and 8 show that this was not the case during metamorphism of carbonate rocks of the Waterville Formation. Interaction of carbonate rocks with aqueous fluid was an essential element of their chemical and mineralogical evolution during the metamorphic event. As a prelude to calculations of how much fluid was involved, the general

Table 8. Mineral-fluid reactions during metamorphism of representative carbonate rocks of each type of mineral assemblage from each outcrop

Sample	Mineral-fluid reaction
	Transition from assemblage A to assemblage B
7-G1	0.081 muscovite + 0.118 ankerite + 1.197 calcite + 2.357$NaAlSi_3O_8$ + 2.359HCl = 0.086 biotite + 4.661 quartz + 1.205$CaAl_2Si_2O_8$ + 0.007 chlorite + 1.433CO_2 + 1.147H_2O + 2.359NaCl
425-E1	0.682 muscovite + 1.856 ankerite + 0.530$NaAlSi_3O_8$ + 0.566HCl = 0.783 biotite + 1.375 calcite + 0.580$CaAl_2Si_2O_8$ + 0.378 quartz + 2.337CO_2 + 0.182H_2O + 0.566NaCl
160-D	0.143 muscovite + 0.407 ankerite + 0.420$NaAlSi_3O_8$ + 0.427HCl = 0.156 biotite + 0.157 calcite + 0.717 quartz + 0.264$CaAl_2Si_2O_8$ + 0.010 chlorite + 0.657CO_2 + 0.161H_2O + 0.427NaCl
5-AA2	0.465 muscovite + 1.264 ankerite + 0.288$NaAlSi_3O_8$ + 0.305HCl = 0.488 biotite + 0.975 calcite + 0.165 quartz + 0.373$CaAl_2Si_2O_8$ + 0.017 chlorite + 1.533CO_2 + 0.061H_2O + 0.305NaCl
1200-B	0.306 muscovite + 0.857 ankerite + 0.389$NaAlSi_3O_8$ + 0.396HCl = 0.325 biotite + 0.609 calcite + 0.481 quartz + 0.347$CaAl_2Si_2O_8$ + 0.017 chlorite + 1.105CO_2 + 0.112H_2O + 0.396NaCl
425-K1	0.748 muscovite + 1.933 ankerite + 2.520$NaAlSi_3O_8$ + 2.559HCl = 0.808 biotite + 0.350 calcite + 4.394 quartz + 1.632$CaAl_2Si_2O_8$ + 3.516CO_2 + 1.219H_2O + 2.559NaCl
5-DD2	1.152 muscovite + 3.242 ankerite + 1.291$NaAlSi_3O_8$ + 1.340HCl = 1.269 biotite + 2.238 calcite + 1.492 quartz + 1.224$CaAl_2Si_2O_8$ + 4.246CO_2 + 0.553H_2O + 1.340NaCl
1200-G	0.741 muscovite + 1.738 ankerite + 0.563$NaAlSi_3O_8$ + 0.596HCl = 0.742 biotite + 1.109 calcite + 0.427 quartz + 0.730$CaAl_2Si_2O_8$ + 2.457CO_2 + 0.297H_2O + 0.596NaCl
3-D1	1.155 muscovite + 2.638 ankerite + 0.377$NaAlSi_3O_8$ + 0.198 quartz + 0.434HCl = 1.106 biotite + 1.808 calcite + 0.909$CaAl_2Si_2O_8$ + 3.468CO_2 + 0.266H_2O + 0.434NaCl
	Transition from assemblage B to assemblage C
425-K1	0.041 biotite + 3.978 ankerite + 3.150 quartz + 0.872$CaAl_2Si_2O_8$ + 0.255$NaAlSi_3O_8$ + 0.856H_2O = 0.897 amphibole + 3.579 calcite + 4.377CO_2
5-DD2	0.007 biotite + 1.342 ankerite + 1.054 quartz + 0.233$CaAl_2Si_2O_8$ + 0.055$NaAlSi_3O_8$ + 0.400H_2O = 0.235 amphibole + 1.267 calcite + 0.043 chlorite + 1.417CO_2
1200-G	0.009 biotite + 0.629 ankerite + 0.898 quartz + 0.026$CaAl_2Si_2O_8$ + 0.013$NaAlSi_3O_8$ + 0.122H_2O = 0.131 amphibole + 0.393 calcite + 0.865CO_2
3-D1	0.010 biotite + 0.798 ankerite + 1.066 quartz + 0.036$CaAl_2Si_2O_8$ + 0.019$NaAlSi_3O_8$ + 0.154H_2O = 0.164 amphibole + 0.530 calcite + 1.066CO_2
	Transition from assemblage C to assemblage D
3-D1	0.780 biotite + 1.743 calcite + 3.799 quartz + 0.075$NaAlSi_3O_8$ = 1.244 diopside + 0.764 K-feldspar + 0.073 clinozoisite + 0.152 amphibole + 0.076$CaAl_2Si_2O_8$ + 0.027 sphene + 0.592H_2O + 1.743CO_2

Note: Reactions refer to mass transfer in 1-L metamorphic rock.

features of mineral reaction and fluid-rock interaction in the carbonate rocks are discussed.

Regardless of bulk composition, rocks from the limestone member of the Waterville Formation apparently contained the same mineral assemblage before biotite developed: ankerite + calcite + albite + quartz + muscovite with combinations of accessory pyrite, pyrrhotite, graphite, rutile, and chlorite (assemblage A). At 400–500°C, a CO_2-H_2O fluid with $X_{CO_2} < \sim 0.05$ is not in chemical equilibrium with this mineral assemblage (see Fig. 2). Therefore when fluid with $X_{CO_2} < \sim 0.05$ gained access to the carbonate rocks, ankerite, albite, and muscovite reacted with it to form biotite, calcite, quartz, An, and a small quantity of chlorite (i.e., assemblage B developed from assemblage A). In almost all specimens the reaction liberated much more CO_2 than H_2O. The difference between the CO_2-rich composition of the volatile mixture released by the reaction and the H_2O-rich fluid with which the samples were in equilibrium during reaction requires that interaction between rock and fluid occurred at all times during the progress of the reaction. The principal chemical variation in mineral solid solutions during the reaction from assemblage A to assemblage B was Fe/(Fe + Mg) (cf., Ferry, 1979). Because of the fractionation of Fe and Mg between ankerite and biotite (Ferry, 1979, Table 1C), Fe/(Fe + Mg) of both biotite and ankerite decreased as the reaction progressed. As mineral compositions changed, the X_{CO_2} of fluid coexisting with the minerals also changed. Judging from the range in measured Fe/(Fe + Mg) of coexisting biotite and ankerite, the maximum change in Fe/(Fe + Mg) was <0.2. Using Figure 6 of Ferry (1979), a change in Fe/(Fe + Mg) of biotite by 0.2 corresponds to a change in X_{CO_2} of ~11% relative (0.01–0.02 at X_{CO_2} = 0.1–0.2). Changes in fluid composition caused by progress of the reaction were negligible.

Because the assemblage amphibole + ankerite is observed in the metacarbonate rocks but never amphibole + muscovite, the transition from assemblage A to assemblage B was complete when muscovite was consumed by the reaction. At this stage, rocks contained ankerite, calcite, quartz, plagioclase, and biotite with various combinations of accessory pyrite, pyrrhotite, rutile, graphite, and chlorite. At 400–500°C, this assemblage is not in chemical equilibrium with CO_2–H_2O fluid with $X_{CO_2} < \sim 0.05$ (see Fig. 2). With further interaction between rock and fluid with $X_{CO_2} < \sim 0.05$, ankerite, quartz, and plagioclase reacted to form calcite and calcic amphibole (i.e., assemblage C developed from assemblage B). Regardless of the temperature of the transition from as-

semblage B to assemblage C, the composition of the fluid with which the rocks were in equilibrium was not greatly different from the composition of the fluid with which the rocks were in equilibrium during the transition from A to B (stippled and black bands in Figure 2 overlap or are closely spaced). The B → C reaction liberated CO_2 and consumed a small amount of H_2O. Because of the difference in composition between the volatiles released by the reaction and the fluid that the rocks were in equilibrium with, interaction between rock and fluid must have occurred throughout the progress of the reaction. The principal chemical variation in mineral solid solutions during the reaction from assemblage B to assemblage C was Fe/(Fe + Mg) (cf., Ferry, 1979). Because of the fractionation of Fe and Mg between amphibole and ankerite (Ferry, 1979, Table 1C), Fe/(Fe + Mg) of both ankerite and amphibole decreased with progress of the reaction. As the compositions of the minerals changed, the X_{CO_2} of coexisting fluid also changed. Judging from the range in measured Fe/(Fe + Mg) of amphibole, the maximum change in Fe/(Fe + Mg) was <0.2. Using Figure 6 of Ferry (1979), a change in Fe/(Fe + Mg) of 0.2 in amphibole corresponds to a change in X_{CO_2} by ~8% relative (0.01–0.02 for X_{CO_2} = 0.1–0.2). Changes in fluid composition caused by progress of the reaction were negligible.

The transition from assemblage B to assemblage C was complete when ankerite was consumed by reaction. At this stage, rocks were composed of biotite, calcic amphibole, calcite, plagioclase, and quartz with various combinations of accessory pyrite, pyrrhotite, rutile, ilmenite, sphene, graphite, and chlorite. At 450–500°C this assemblage is not in chemical equilibrium with CO_2–H_2O fluid with $X_{CO_2} < \sim 0.05$ (see Fig. 2). With further interaction between carbonate rock and fluid with $X_{CO_2} < \sim 0.05$, biotite, calcite, and quartz reacted to form diopside, K-feldspar, and clinozoisite (i.e., assemblage D developed from assemblage C). The reaction liberated a CO_2-rich mixture of volatiles yet the minerals were in equilibrium with an H_2O-rich fluid with $X_{CO_2} < 0.1$; interaction between rock and fluid must have occurred throughout the progress of the reaction. The small range in calculated X_{CO_2} of fluid in equilibrium with all analyzed samples of assemblage D (Table 6) suggests that changes in fluid composition caused by progress of the reaction were negligible.

Only samples with assemblage D from outcrop 3 experienced the entire sequence of reactions; all other samples experienced only part of it. Nevertheless, three generalizations may be made about fluid compositions and fluid-rock interaction during metamorphism of the limestone member of the Waterville Formation. First, changes in fluid composition caused by progress of all prograde reactions were negligible (<0.02 X_{CO_2}). Furthermore, regardless of the temperature at which muscovite was consumed and calcic amphibole began to form, fluid composition changed very little as the biotite-forming reaction was replaced by the amphibole-forming reaction (Fig. 2). Second, chemical interaction between carbonate rock and fluid occurred at all times during metamorphism while prograde devolatilization reactions were proceeding. Third, all observed mineral assemblages in the carbonate rocks would be out of chemical equilibrium with CO_2-H_2O fluid with $X_{CO_2} < \sim 0.05$ at 400–500°C. Consequently, infiltration of rock by such fluid at all stages in the metamorphism of the metacarbonates resulted in mineral-fluid reaction. Conversely, CO_2-H_2O fluid with $X_{CO_2} <$ 0.05 could not have infiltrated carbonate rock at any stage without leaving a record of mineral-fluid reaction.

Calculated fluid-rock ratios: Method and assumptions

If the composition of the fluid that interacted with carbonate rock during metamorphism can be estimated or assumed, if it is assumed that fluid rapidly attained chemical equilibrium with rock during metamorphic fluid-rock interaction, if the composition of fluid with which the rock was in equilibrium did not significantly change during reaction, and if the amount of volatiles released by the metamorphic reactions can be determined, then the amount of fluid with which a particular rock sample interacted can be estimated (Ferry, 1986a):

$$X^{eq}_{CO_2} = [(X^{infilt}_{CO_2} n_T) + n^{rxn}_{CO_2}]/[n^{rxn}_{CO_2} + n^{rxn}_{H_2O} + n_T], \quad (5)$$

where n_i^{rxn} is the number of moles of volatile species i released in a reference quantity of rock during metamorphism, $X^{eq}_{CO_2}$ is the mole fraction of CO_2 in fluid that the rock was in equilibrium with during reaction, $X^{infilt}_{CO_2}$ is the mole fraction of CO_2 in fluid that the rock chemically interacted with, and n_T is the total moles of fluid that the reference quantity of rock interacted with. The effects of HCl and NaCl upon calculated amounts of fluid exactly cancel; terms for n^{rxn}_{HCl} and n^{rxn}_{NaCl} therefore were omitted from Equation 5.

Equation 5 was applied to 67 samples of carbonate rock from the six outcrops of the Waterville Formation located in Figure 1. The entire reaction history of each sample was divided into three stages, corresponding to the transitions between assemblages A and B, between assemblages B and C, and between assemblages C and D, and n_T was calculated for each stage. The various reactions, A → B, B → C, and C → D, occurred in particular samples over small ranges in temperature and hence $X^{eq}_{CO_2}$ (see Fig. 2). In order to apply Equation 5, however, some estimate must be made of the value of temperature and hence $X^{eq}_{CO_2}$ at which CO_2 was produced by the reactions and at which H_2O was produced or consumed. The estimated values are summarized in Table 9. The cumulative number of moles of fluid with which rock samples interacted during metamorphism was estimated as the sum of the n_T values calculated for each stage. The composition of fluid that interacted with the rocks was assumed to be H_2O ($X^{infilt}_{CO_2} = 0$; $n_T = n_{H_2O}$). The reference quantity of rock was chosen as 1 L after metamorphism. The amount of CO_2 and H_2O liberated by each rock sam-

Table 9. Estimated temperature and composition of metamorphic fluid during mineral-fluid reaction in each type of mineral assemblage from each outcrop

Outcrop	Assemblage transition	Temperature of reaction	$X^{eq}_{CO_2}$ during reaction
7	A → B	390°C	0.07
425	A → B	410°C	0.06
425	B → C	410°C	0.07
160	A → B	430°C	0.11
5	A → B	440°C	0.12
5	B → C	450°C	0.16
1200	A → B	440°C	0.12
1200	B → C	460°C	0.18
3	A → B	440°C	0.12
3	B → C	460°C	0.18
3	C → D	530°C	0.10

ple at each stage of reaction was taken directly from the reconstructed prograde sequence of reactions (data like those in Table 8). Moles of H_2O calculated from Equation 5 were converted to a volume of H_2O using molar-volume data (Burnham et al., 1969) to estimate a volumetric fluid-rock ratio for each sample. Calculated results are summarized in Figures 4–11.

Fluid-rock ratios calculated from Equation 5 have errors determined by errors in $X^{eq}_{CO_2}$, $X^{infilt}_{CO_2}$, $n^{rxn}_{CO_2}$, and $n^{rxn}_{H_2O}$. Errors in $X^{eq}_{CO_2}$, $X^{infilt}_{CO_2}$, $n^{rxn}_{CO_2}$, and $n^{rxn}_{H_2O}$ are, in turn, the result of errors in modal analysis, in electron-microprobe analysis, whole-rock chemical analysis, thermochemical data for mineral equilibria, fugacity and activity coefficients for fluid species, and activity-composition relationships among minerals. Errors in calculated fluid-rock ratios therefore could, in principle, be estimated by propagating errors in these quantities through calculations of $X^{eq}_{CO_2}$, $X^{infilt}_{CO_2}$, $n^{rxn}_{CO_2}$, and $n^{rxn}_{H_2O}$ and by propagating errors in $X^{eq}_{CO_2}$, $X^{infilt}_{CO_2}$, $n^{rxn}_{CO_2}$, and $n^{rxn}_{H_2O}$ in turn, through Equation 5. Unfortunately, some of the sources of error in calculations of $X^{eq}_{CO_2}$, $X^{infilt}_{CO_2}$, $n^{rxn}_{CO_2}$, and $n^{rxn}_{H_2O}$ do not readily lend themselves to quantitative analysis. The errors associated with calculated fluid-rock ratios therefore were semiquantitatively assessed in two other ways. First, a general comparison may be made between fluid-rock ratios calculated in other studies from equations analogous to Equation 5 and fluid-rock ratios estimated from stable-isotope data for the same rocks. The two types of fluid-rock ratio commonly agree within ~25–50% relative (Ferry, 1986b); calculated results in this study, by analogy, may be accurate within approximately 25–50% relative or better.

Second, errors in calculated fluid-rock ratio may be explored by examining the dependence of fluid-rock ratio on values of $X^{eq}_{CO_2}$ and $X^{infilt}_{CO_2}$ in Equation 5. Figure 3 illustrates the effect of varying $X^{eq}_{CO_2}$ and $X^{infilt}_{CO_2}$ on calculated fluid-rock ratio for one typical sample that experienced only the reaction corresponding the transition between assemblages A and B [sample (a), Fig. 6]. The preferred estimate of fluid-rock ratio (0.50) is conservative in the sense that the value of $X^{infilt}_{CO_2}$ was taken as 0. If $X^{infilt}_{CO_2} > 0$, the calculated fluid-rock ratio would be greater than 0.50. If $X^{infilt}_{CO_2}$ were greater than $X^{eq}_{CO_2}$, however, fluid-rock reaction would have resulted in carbonation of rock rather than the observed decarbonation reaction. Consequently $X^{infilt}_{CO_2}$ must have been less than $X^{eq}_{CO_2}$ (0.12 at 440°C). If $X^{infilt}_{CO_2}$ were less than $X^{eq}_{CO_2}$ but within ~0.02 of it, Figure 3 clearly shows that fluid-rock ratios may have been substantially greater than those estimated in Figures 4–11 by a factor of 5–10 or more. If $X^{eq}_{CO_2}$ during the reaction were significantly greater than the preferred estimate of 0.12 (0.25, for example), fluid-rock ratios may have been smaller, by a factor of ~50%, than those estimated here. On the other hand, if $X^{eq}_{CO_2}$ were much less than 0.12 (< ~0.025), fluid-rock ratios may have been much greater than those estimated by a factor of 5 or more.

More important than the absolute value of fluid-rock ratios is the relative proportion of fluid-rock ratios calculated for pairs of samples from the same outcrop (i.e., the ratio of two fluid-rock ratios). The relative proportion of fluid-rock ratios can answer the most important question addressed by this study: whether fluid flow was pervasive (relative proportions uniform within each outcrop) or channelized during metamorphism (relative proportions variable within each outcrop). The value of $X^{eq}_{CO_2}$ probably differed by <0.02 at all times during metamorphism within individual outcrops. It is unlikely that the infiltrating fluid differed in composition from bed to bed within individual outcrops during the metamorphic event. Consider two samples (denoted by superscripts a and b) that interact with aqueous fluid of the same $X^{infilt}_{CO_2}$ and that are in equilibrium with fluid with the same $X^{eq}_{CO_2}$. If the resulting mineral-fluid reaction liberates much more CO_2 than H_2O, i.e., if $n^{rxn}_{CO_2} \gg n^{rxn}_{H_2O}$, as evidently was the case during metamorphism of the limestone member of the Waterville Formation (cf., Table 8), then from Equation 5,

$$(n_T)^a/(n_T)^b = \frac{X^{eq}_{CO_2}[(n^{rxn}_{CO_2})^a + (n^{rxn}_{H_2O})^a] - (n^{rxn}_{CO_2})^a}{X^{eq}_{CO_2}[(n^{rxn}_{CO_2})^b + (n^{rxn}_{H_2O})^b] - (n^{rxn}_{CO_2})^b}$$

$$\approx (n^{rxn}_{CO_2})^a/(n^{rxn}_{CO_2})^b. \quad (6)$$

Under such circumstances, the relative proportion of fluid-rock ratios is, for practical purposes, the same as the ratio between the number of moles CO_2 released by two samples during reaction. Errors in the absolute value of an individual fluid-rock ratio, introduced by errors in estimated values for $X^{eq}_{CO_2}$ and $X^{infilt}_{CO_2}$, cancel out in the consideration of the relative proportion of fluid-rock ratios. If estimated fluid-rock ratios for a single outcrop are in error, they all err in the same direction and by an amount proportional to the estimated value. Consequently, the ratio of any two fluid-rock ratios for the same outcrop may be read from Figures 4–11 with much greater accuracy than estimates of the fluid-rock ratio for individual samples.

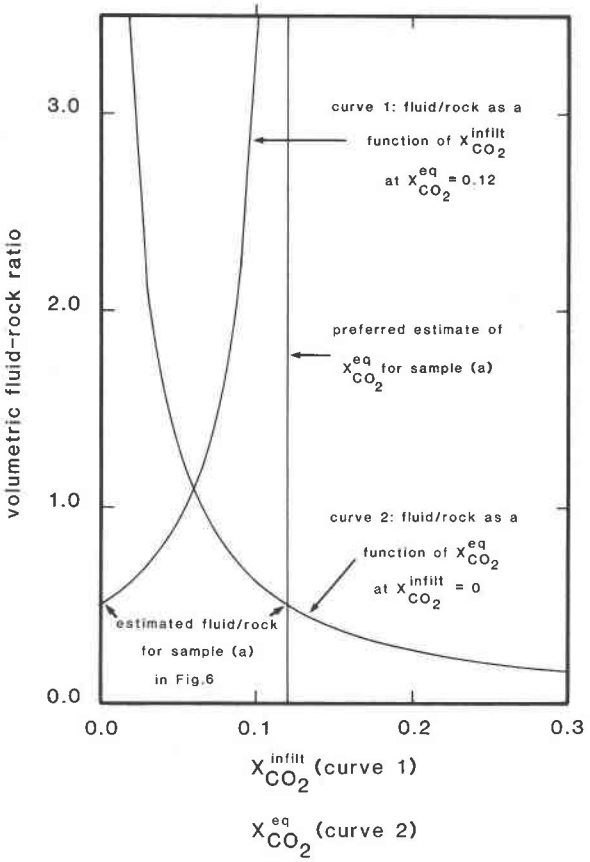

Fig. 3. Effect of varying $X^{eq}_{CO_2}$ and $X^{infilt}_{CO_2}$ in Eq. 5 on calculated fluid-rock ratio for sample (a), Fig. 6.

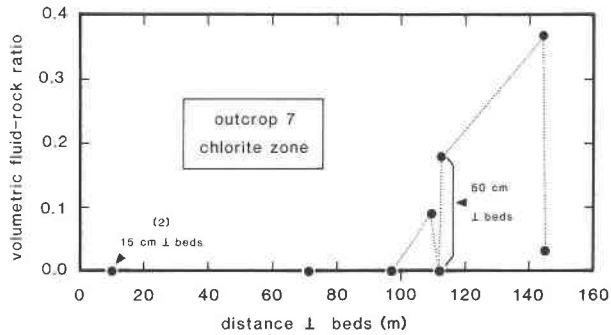

Fig. 4. Calculated fluid-rock ratios for samples collected along a traverse across bedding in outcrop 7. Each data point refers to a single sample except where noted by small number in parentheses. Separation of closely spaced samples given in centimeters.

Calculated fluid-rock ratios: Results

Outcrop 7. Fluid-rock ratios calculated for samples from outcrop 7 are plotted against distance perpendicular to bedding in Figure 4. In the chlorite zone there are significant differences in calculated fluid-rock ratios between different beds. Five of nine samples record fluid-rock ratios of zero; four samples record fluid-rock ratios of 0.03–0.37. Gradients in fluid-rock ratio with distance perpendicular to beds may be large. At a distance of ~110 m along the trasverse, two beds separated by 7 m parallel to bedding and 0.5 m perpendicular to bedding record fluid-rock ratios that differ by ~0.19. At a distance of ~145 m along the traverse, two beds separated by 3 m parallel to bedding and by 1 m perpendicular to bedding record fluid-rock ratios that differ by ~0.36.

Outcrop 425. Four samples from outcrop 425 were studied in detail along a traverse ~20 m perpendicular to bedding. Only those rocks that showed significant degrees of reaction were collected in the outcrop (i.e., rocks with visibly abundant biotite and/or amphibole), and consequently the four samples are not representative of the outcrop as a whole. The four calculated fluid-rock ratios are 0.63, 0.76, 1.51, and 2.37. Results show that significantly more fluid passed through at least some beds metamorphosed to conditions of the biotite zone than passed through any of the rocks collected from the chlorite zone. Too few samples were collected from outcrop 425 to map the distribution of fluid-rock ratios.

Outcrop 160. Fluid-rock ratios calculated for nine samples from outcrop 160 and plotted at their position along a traverse ~15 m perpendicular to bedding are shown in Figure 5. Two beds at 5 and 17 m along the traverse record large fluid-rock ratios, 1.1–1.5. All other beds record small fluid-rock ratios, 0.02–0.12. More than one sample was collected along strike within several beds including both beds that record high fluid-rock ratios and beds that record low fluid-rock ratios. Three samples collected over a distance of 14 m within the bed at 16 m

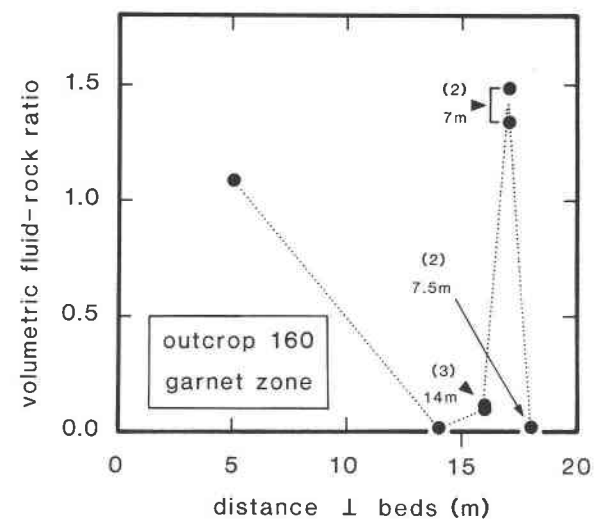

Fig. 5. Calculated fluid-rock ratios for samples collected along a traverse across bedding in outcrop 160. Each data point refers to a single sample except where noted by small numbers in parentheses. Other small numbers refer to the separation in the horizontal direction parallel to bedding of samples collected from the same bed.

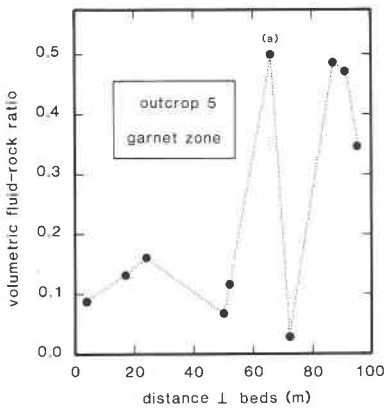

Fig. 6. Calculated fluid-rock ratios for samples collected along a traverse across bedding in outcrop 5. Same traverse as in Fig. 7 of Ferry (1979). Each data point refers to a single sample from a different bed.

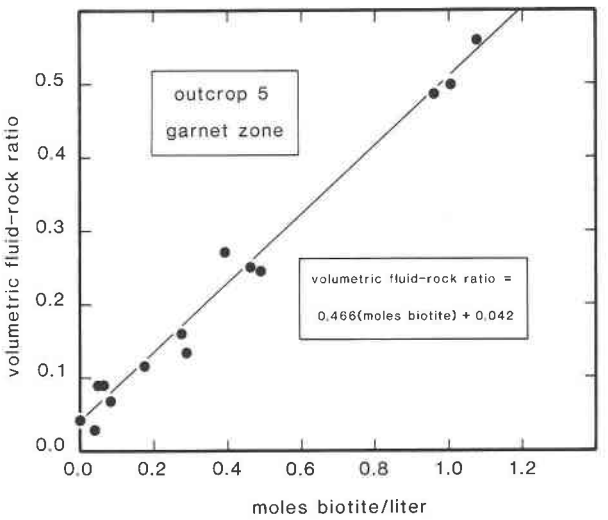

Fig. 8. Calculated volumetric fluid-rock ratio plotted against molar biotite content (moles/liter) for rocks with assemblage B from outcrop 5. Equation is a linear least-squares fit to the data points.

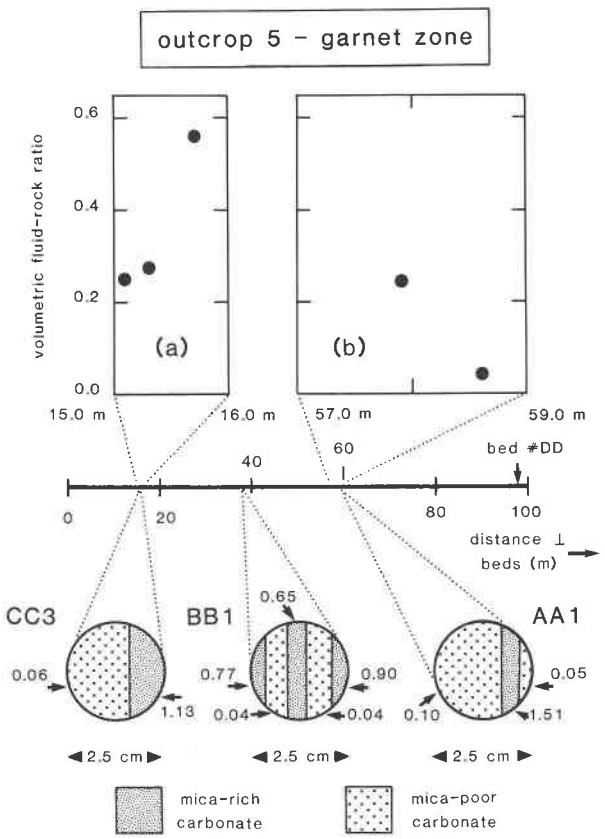

Fig. 7. Calculated fluid-rock ratios for samples collected along a traverse across bedding in outcrop 5 located approximately 200 m south of the traverse in Fig. 6. Each data point refers to a single sample. Circles at bottom of figure are sketches of three thin sections of carbonate rock containing alternating thin mica-rich and mica-poor layers. Small numbers by sketches are volumetric fluid-rock ratios estimated for mica-rich and mica-poor portions of each sample.

along the traverse record fluid-rock ratios of 0.09, 0.11, and 0.12. Two samples collected 7.5 m apart within the same bed at 18 m along the traverse record fluid-rock ratios of 0.02 and 0.03. Two samples collected 7 m apart within the same bed at 17 m along the traverse record fluid-rock ratios of 1.34 and 1.50. Calculated fluid-rock ratios are constant or relatively constant within each bed over distances of at least 14 m. Fluid-rock ratios, however, may differ by a factor of ~60 between different beds only 1 m distant perpendicular to strike. At least small amounts of fluid have chemically interacted with all beds of outcrop 160. Most beds record fluid-rock ratios of $< \sim 0.2$. Much more fluid, however, reacted with a few of the beds in the outcrop.

Outcrop 5. Fluid-rock ratios were calculated for 19 samples from outcrop 5 along several traverses both perpendicular and parallel to bedding, and results are illustrated in Figures 6–9. All specimens collected over a distance of ~100 m along one traverse (Fig. 6) chemically interacted with 0.03–0.50 rock volumes of H_2O fluid. Most samples record low fluid-rock ratios in the narrow range of 0.03–0.15. The remaining samples record significantly higher fluid-rock ratios, 0.35–0.50. As in outcrop 160, fluid-rock ratios are not uniform throughout the outcrop but may vary by over a factor of 10 between beds located a few meters apart perpendicular to bedding.

The scale of the variation in fluid-rock ratio perpendicular to bedding was investigated with samples collected along a second traverse perpendicular to bedding. Results are summarized in Figure 7. As along the traverse in Figure 6, calculated fluid-rock ratios vary by over a factor of ten (0.04–1.51) from bed to bed over distances of tens of meters. Similar differences in fluid-rock ratio occur on a scale of centimeters. Along subsection (a), Figure 7, for example, calculated fluid-rock ratios are be-

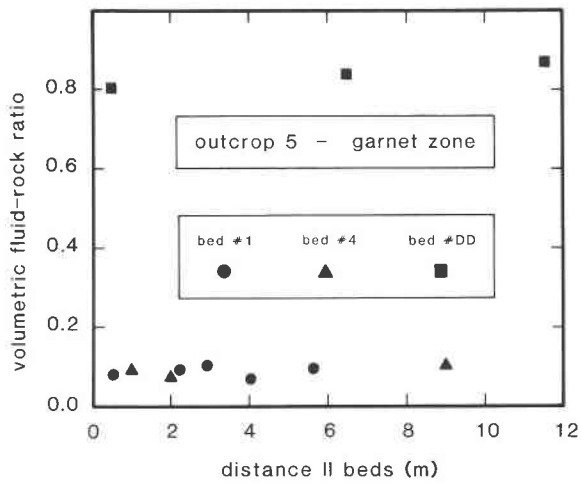

Fig. 9. Calculated fluid-rock ratios for samples collected along three traverses parallel to bedding in outcrop 5 (beds 1, 4, and DD). Beds 1 and 4 are the same as those in Figs. 8 and 10, respectively, of Ferry (1979). Bed DD is located relative to other samples in Fig. 7. Each data point refers to a single sample.

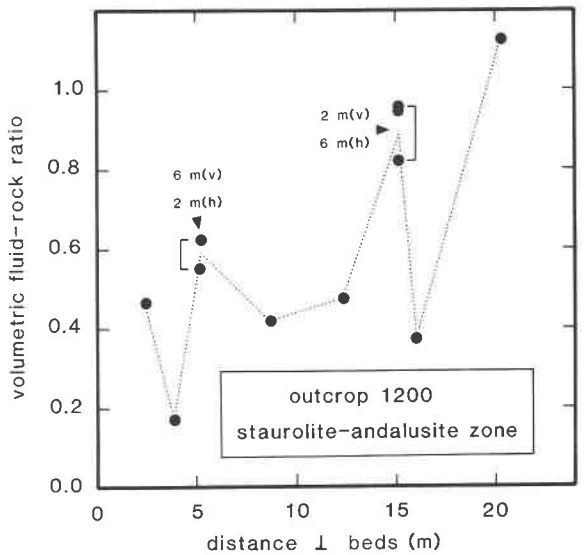

Fig. 10. Calculated fluid-rock ratio for samples collected along a traverse across bedding in outcrop 1200. Each data point refers to a single sample. For samples from the same bed (same distance along traverse), small numbers refer to their separation in both the vertical (v) and horizontal (h) directions parallel to bedding.

tween 0.25 and 0.56 in samples located 40 cm apart perpendicular to bedding. Along subsection (b), fluid-rock ratios are between 0.04 and 0.25 in samples located 70 cm apart perpendicular to bedding.

Variations in fluid-rock ratio on an even finer scale were investigated with three samples located at 15, 38, and 58 m along the traverse in Figure 7. In thin sections of the three specimens, mica-rich carbonate layers alternate with mica-poor carbonate layers. All layers are homogeneous and contain assemblage B but with different proportions of minerals. The boundaries between the layers are remarkably sharp with the transition from mica-rich to mica-poor regions occurring over a distance of 0.5–1 mm. The amount of biotite in each layer was determined by counting 1000–2000 points in thin section. A fluid-rock ratio was estimated for each layer from an empirical linear relationship between fluid-rock ratio and molar biotite content of all other samples from outcrop 5 that contain assemblage B (Fig. 8). In sample AA1, fluid-rock ratios are between 0.05 and 1.51 over a distance of <1 mm. Over the same distance in samples BB1 and CC3, fluid-rock ratios are between 0.04 and 0.90 and between 0.06 and 1.13, respectively.

Variations in fluid-rock ratio along beds in outcrop 5 were investigated in three individual beds. Results are illustrated in Figure 9. Calculated fluid-rock ratios are effectively constant for distances of at least 12 m along each bed. Fluid-rock ratios are uniformly low along both beds 1 and 4, 0.06–0.10 and 0.07–0.10, respectively. Fluid-rock ratios are uniformly high along bed DD, 0.79–0.86.

The geometric pattern of fluid-rock ratios in outcrop 5 is regular and bears a simple relationship to bedding. Calculated fluid-rock ratios vary between different beds, ranging from 0.03 to 1.51 on scales of millimeters to tens of meters perpendicular to bedding. In contrast to relations perpendicular to bedding, no significant variation in fluid-rock ratio was detected over distances of up to 12 m within any bed parallel to bedding. Fluid-rock ratio appears to be constant within each bed. The pattern of fluid-rock ratios is closely analogous to the geometric pattern of the chemical potentials of volatiles in the outcrop during metamorphism (Ferry, 1979). Significant differences in the chemical potentials of CO_2 and H_2O occurred in the outcrop between beds several meters distant perpendicular to bedding, but no significant chemical-potential differences were detected within beds over distances of up to 10 m parallel to bedding.

Outcrop 1200. Fluid-rock ratios calculated for 11 samples collected from outcrop 1200 and plotted along a traverse perpendicular to bedding are shown in Figure 10. Calculated fluid-rock ratios differ from bed to bed in the range of 0.17–1.13 over distances of ~20 m perpendicular to bedding. As at lower grades, fluid-rock ratios are not significantly different between samples collected from the same bed. Within the same bed located 5 m along the traverse, for example, two samples, separated by 2 m horizontally and 6 m vertically, record fluid-rock ratios of 0.54 and 0.62. Three samples within the same bed located 15 m along the traverse, separated by 6 m horizontally and 2 m vertically, record fluid-rock ratios of 0.81, 0.93, and 0.94. There are, however, two differences between outcrop 1200 and the outcrops at lower grades: (1) the average fluid-rock ratio is greater in outcrop 1200 than at lower grades (cf., Fig. 10 with Figs. 4, 5, and 6), and (2) the differences in calculated fluid-rock ratios between beds are less in outcrop 1200 than at lower grades

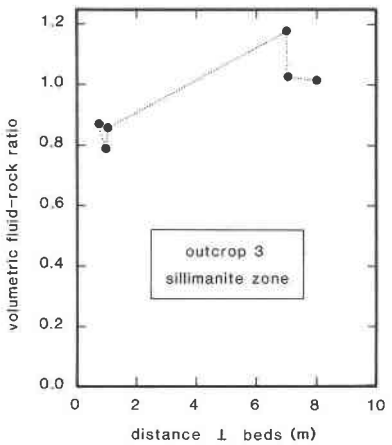

Fig. 11. Calculated fluid-rock ratio for samples collected along a traverse across bedding in outcrop 3. Each data point refers to a single sample.

(fluid-rock ratio varies by no more than a factor of ~6 in outcrop 1200 compared to a factor of ~50 in outcrop 5 and a factor of ~60 in outcrop 160).

Outcrop 3. Fluid-rock ratios for 6 samples collected from outcrop 3 and plotted along a traverse perpendicular to bedding are shown in Figure 11. Calculated fluid-rock ratios differ from bed to bed in the range of 0.78–1.18 over a distance of 7 m perpendicular to bedding. Two samples collected 5 cm apart perpendicular to bedding approximately 1 m along the traverse are mica-rich and mica-poor yet record fluid-rock ratios of 0.78 and 0.86, respectively. Two samples collected 5 cm apart perpendicular to bedding approximately 8 m along the traverse record fluid-rock ratios of 1.02 and 1.18. Fluid-rock ratios varied between beds on a scale of meters but not significantly between different lithologic layers on a scale of centimeters during metamorphism at outcrop 3. Compared to outcrops at lower grades (1) average fluid-rock ratios are greater in outcrop 3, and (2) differences in fluid-rock ratios between beds are much less (fluid-rock ratios vary by no more than a factor of ~1.5 compared to factors of ~6, ~50, and ~60 in outcrops at lower grades).

Discussion

Pattern of fluid flow during regional metamorphism

Because all observed mineral assemblages from the limestone member of the Waterville Formation were out of chemical equilibrium with CO_2-H_2O fluid with $X_{CO_2} <$ ~0.05 at the P-T conditions of metamorphism, all fluid that flowed through the rocks chemically reacted with them, if kinetics permitted. The rates of hydrothermal reactions are sufficiently rapid that kinetics probably did not prohibit any mineral-fluid reaction during the metamorphic event (Walther and Wood, 1984). As a corollary, therefore, the observed reactions in the metacarbonate rocks record, through Equation 5, the amount of all reactive fluid that flowed through the rocks (i.e., all fluid except for any fluid that had precisely the composition to be in chemical equilibrium with the carbonate rocks). The pattern of calculated fluid-rock ratios at each outcrop, therefore, mimics the flow pattern of reactive fluid through the outcrop during the metamorphic event. Regions of high flow of reactive fluid correspond in outcrop to individual lithologic layers. Evidently flow was highly channelized with enhanced fluid flow along some beds that acted as metamorphic aquifers and reduced fluid flow along other beds that acted as metamorphic aquitards. Flow of reactive fluid evidently was uniform within each individual bed (cf., Figs. 5 and 9). The nonzero fluid-rock ratios calculated for every sample collected in the biotite zone and at higher grades, however, indicate that there was a small component of pervasive flow that permeated all metacarbonate rocks during the metamorphic event.

The pattern of flow of reactive fluid during regional metamorphism of impure carbonate rocks from the Waterville Formation is the same as the pattern of fluid flow during contact metamorphism of impure carbonate rocks around the Notch Peak granite, Utah (Nabelek et al., 1984). Nabelek et al. used stable-isotope data to show that fluid flow in the Cambrian Orr Formation was channelized almost exclusively along certain stratigraphic horizons. The intervening beds acted as relatively impermeable aquitards. Similarly, Rye et al. (1976) concluded from stable-isotope data that fluid flow was highly channelized during regional metamorphism on Naxos into pelitic interbeds and/or along contacts between pelites and massive limestones. The limestones acted as less-permeable aquitards. The stable-isotope data of Rye et al. (1976), moreover, suggest that fluid flux through the limestones increased with increasing grade, in harmony with the results of this study. The flow of fluid during contact and regional metamorphism, at least in some instances, is evidently closely analogous to the movement of groundwater through rocks closer to the Earth's surface.

The pattern of fluid flow during regional metamorphism of the limestone member of the Waterville Formation, on the other hand, appears to have been quite different from the pattern of fluid flow through pelitic rocks that compose the bulk of the formation. Pelitic phyllites from the biotite zone of the Waterville Formation record chemical interaction with 1–2 rock volumes of H_2O fluid during the mineral reaction by which biotite developed in them (Ferry, 1984). Because volumetric fluid-rock ratios calculated for seven samples of pelite from five different outcrops are in the relatively narrow range 1–2, flow of reactive fluid appears to have been much more pervasive in the phyllites during metamorphism than in the massive metacarbonate rocks. Because of the difference in lithology between the limestone member of the Waterville Formation and the rest of the unit, however, there is no reason to expect that patterns of fluid flow should be the same. Permeability variations of several orders of magnitude can occur between different rock types on a scale commensurate with sedimentary layering; there are consequent variations in the flow pattern of groundwater on the same scale (Freeze and Cherry,

1979; Brace, 1980, 1984). It appears that differences in permeability and in patterns of fluid flow occur on a similar scale during regional metamorphism as controlled by variations in the physical properties of different sedimentary units.

Effect of metamorphic grade on the pattern of fluid flow during metamorphism

Judging from the calculated fluid-rock ratios in Figures 4–11, the effect of increasing metamorphic grade on the patterns of flow of reactive fluid evidently is twofold: (1) the flux of reactive fluid that flowed through rocks increased with grade of metamorphism (average fluid-rock ratios increase with increasing metamorphic grade); and (2) fluid flow was much more pervasive during high-grade metamorphism than during low-grade metamorphism (the variation in fluid-rock ratio within an outcrop decreases dramatically with increasing metamorphic grade).

Acknowledgments

Research supported by a Cottrell Grant from Research Corporation and grants EAR 82-18464 and EAR 84-20889, Earth Sciences Division, National Science Foundation. Thoughtful reviews from T. C. Labotka, L. C. Pigage, and J. M. Rice are gratefully appreciated; conclusions, however, may not represent those of the reviewers.

References

Allen, J.M., and Fawcett, J.J. (1982) Zoisite-anorthite-calcite stability relations in H_2O-CO_2 fluids at 5000 bars: An experimental and SEM study. Journal of Petrology, 23, 215–239.

Bebout, G.E., and Carlson, W.D. (1986) Fluid evolution and transport during metamorphism: Evidence from the Llano uplift, Texas. Contributions to Mineralogy and Petrology, 92, 518–529.

Brace, W.F. (1980) Permeability of crystalline and argillaceous rocks. International Journal of Rock Mechanics and Mining Science, 17, 241–251.

——— (1984) Permeability of crystalline rocks: New in situ measurements. Journal of Geophysical Research, 89, 4327–4330.

Burnham, C.W., Holloway, J.R., and Davis, N.F. (1969) Thermodynamic properties of water to 1000°C and 10,000 bars. Geological Society of America Special Paper 132.

Carmichael, D.M. (1969) On the mechanism of prograde metamorphic reactions in quartz-bearing pelitic rocks. Contributions to Mineralogy and Petrology, 20, 244–267.

Carpenter, M.A., and Ferry, J.M. (1984) Constraints on the thermodynamic mixing properties of plagioclase feldspars. Contributions to Mineralogy and Petrology, 87, 138–148.

Dallmeyer, R.D., and Van Breeman, O. (1981) Rb-Sr whole-rock and $^{40}K/^{39}Ar$ mineral ages of the Togus and Hallowell quartz monzonite and Three Mile Pond granodiorite plutons, south-central Maine: Their bearing on post-Acadian cooling history. Contributions to Mineralogy and Petrology, 78, 61–73.

Ferry, J.M. (1976) *P, T,* f_{CO_2} and f_{H_2O} during metamorphism of calcareous sediments in the Waterville-Vassalboro area, south-central Maine. Contributions to Mineralogy and Petrology, 57, 119–143.

——— (1979) A map of chemical potential differences within an outcrop. American Mineralogist, 64, 966–985.

——— (1980) A comparative study of geothermometers and geobarometers in pelitic schists from south-central Maine. American Mineralogist, 65, 720–732.

——— (1983a) Mineral reactions and element migration during metamorphism of calcareous sediments from the Vassalboro Formation, south-central Maine. American Mineralogist, 68, 334–354.

——— (1983b) Regional metamorphism of the Vassalboro Formation, south-central Maine, U.S.A.: A case study of the role of fluid in metamorphic petrogenesis. Geological Society of London Journal, 140, 551–576.

——— (1983c) On the control of temperature, fluid composition, and reaction progress during metamorphism. American Journal of Science, 283A, 201–232.

——— (1984) A biotite isograd in south-central Maine, U.S.A.: Mineral reactions, fluid transfer, and heat transfer. Journal of Petrology, 25, 871–893.

——— (1986a) Reaction progress: A monitor of fluid-rock interaction during metamorphic and hydrothermal events. In J.V. Walther and B.J. Wood, Eds. Fluid-rock interactions during metamorphism, p. 60–88. Springer-Verlag, New York.

——— (1986b) Infiltration of aqueous fluid and high fluid-rock ratios during greenschist facies metamorphism: A reply. Journal of Petrology, 27, 695–714.

Ferry, J.M., and Burt, D.M. (1982) Characterization of metamorphic fluid composition through mineral equilibria. Mineralogical Society of America Reviews in Mineralogy, 10, 207–262.

Frantz, J.D., Popp, R.K., and Boctor, N.S. (1981) Mineral-solution equilibria—V. Solubilities of rock-forming minerals in supercritical fluids. Geochimica et Cosmochimica Acta, 45, 69–77.

Freeze, R.A., and Cherry, J.A. (1979) Groundwater. Prentice-Hall, Englewood Cliffs, New Jersey.

Grove, T.L., Ferry, J.M., and Spear, F.S. (1983) Phase transitions and decomposition relations in calcic plagioclase. American Mineralogist, 68, 41–59.

Hewitt, D.A. (1973) Stability of the assemblage muscovite-calcite-quartz. American Mineralogist, 58, 785–791.

Hewitt, D.A., and Wones, D.R. (1975) Physical properties of some synthetic Fe-Mg-Al trioctahedral biotites. American Mineralogist, 60, 854–862.

Holdaway, M.J., Guidotti, C.V., Novak, J.M., and Henry, W.E. (1982) Polymetamorphism in medium- to high-grade pelitic metamorphic rocks, west-central Maine. Geological Society of America Bulletin, 93, 572–584.

Hoschek, G. (1973) Die Reaktion Phlogopit + Calcit + Quartz = Tremolit + Kalifeldspat + H_2O + CO_2. Contributions to Mineralogy and Petrology, 39, 231–237.

Jacobs, G.K., and Kerrick, D.M. (1981) Devolatilization equilibria in H_2O-CO_2 and H_2O-CO_2-NaCl fluids: An experimental and thermodynamic evaluation at elevated pressures and temperatures. American Mineralogist, 66, 1135–1153.

Leake, B.E. (1978) Nomenclature of amphiboles. American Mineralogist, 63, 1023–1052.

McOnie, A.W., Fawcett, J.J., and James, R.S. (1975) The stability of chlorites in the clinochlore-daphnite series at 2 kbar P_{H_2O}. American Mineralogist, 60, 1047–1062.

Nabelek, P.I., Labotka, T.C., O'Neil, J.R., and Papike, J.J. (1984) Contrasting fluid/rock interaction between the Notch Peak granitic intrusion and argillites and limestones in western Utah: Evidence from stable isotopes and phase assemblages. Contributions to Mineralogy and Petrology, 86, 25–34.

Novak, J.M., and Holdaway, M.J. (1981) Metamorphic petrology, mineral equilibria, and polymetamorphism in the Augusta Quadrangle, south-central Maine. American Mineralogist, 66, 51–69.

Osberg, P.H. (1968) Stratigraphy, structural geology, and metamorphism of the Waterville-Vassalboro area, Maine. Maine Geological Survey Bulletin 20.

——— (1979) Geologic relationships in south-central Maine. In P.H. Osberg and J.W. Skehan, Eds. The Caledonides in the U.S.A., p. 37–62. Weston Observatory of Boston College, Weston, Massachusetts.

Puhan, D. (1978) Experimental study of the reaction: Dolo-

mite + K-feldspar + H_2O = phlogopite + calcite + CO_2 at the total gas pressures of 4000 and 6000 bars. Neues Jahrbuch für Mineralogie Monatshefte, 3, 110–127.

Rice, J.M., and Ferry, J.M. (1982) Buffering, infiltration, and the control of intensive variables during metamorphism. Mineralogical Society of America Reviews in Mineralogy, 10, 263–326.

Robie, R.A., Bethke, P.M., and Beardsley, K.M. (1967) Selected X-ray crystallographic data, molar volumes, and densities of minerals and related substances. U.S. Geological Survey Bulletin 1248.

Rumble, D., Ferry, J.M., Hoering, T.C., and Boucot, A.J. (1982) Fluid flow during metamorphism at the Beaver Brook fossil locality, New Hampshire. American Journal of Science, 282, 886–919.

Rye, R.O., Schuiling, R.D., Rye, D.M., and Jansen, J.B.H. (1976) Carbon, hydrogen, and oxygen isotope studies of the regional metamorphic complex at Naxos, Greece. Geochimica et Cosmochimica Acta, 40, 1031–1049.

Skippen, G.B. (1974) An experimental model for low pressure metamorphism of siliceous dolomitic marble. American Journal of Science, 274, 487–509.

Thompson, A.B. (1975) Calc-silicate diffusion zones between marble and pelitic schists. Journal of Petrology, 16, 314–346.

Tracy, R.J., Rye, D.M., Hewitt, D.A., and Schiffries, C.M. (1983) Petrologic and stable-isotopic studies of fluid-rock interactions, south-central Connecticut: I. The role of infiltration in producing reaction assemblages in impure marbles. American Journal of Science, 283A, 589–616.

Walther, J.V., and Orville, P.M. (1982) Volatile production and transport in regional metamorphism. Contributions to Mineralogy and Petrology, 79, 252–257.

Walther, J.V., and Wood, B.J. (1984) Rate and mechanism in prograde metamorphism. Contributions to Mineralogy and Petrology, 88, 246–259.

Manuscript received May 14, 1985
Manuscript accepted September 2, 1986